RI 8711

Bureau of Mines Report of Investigations/1982

Performance Evaluation of Electromagnetic Techniques for the Location of Trapped Miners

By John Durkin

UNITED STATES DEPARTMENT OF THE INTERIOR

Report of Investigations 8711

Performance Evaluation of Electromagnetic Techniques for the Location of Trapped Miners

By John Durkin

UNITED STATES DEPARTMENT OF THE INTERIOR
James G. Watt, Secretary

BUREAU OF MINES
Robert C. Horton, Director

This publication has been cataloged as follows:

Durkin, John

Performance evaluation of electromagnetic techniques for the location of trapped miners.

(Report of investigations / United States Department of the Interior, Bureau of Mines ; 8711.

Bibliography: p. 29-30.

Supt. of Docs. no.: I 28.23:8711.

1. Mine rescue work–Equipment and supplies–Evaluation. 2. Electromagnetic fields. 3. Signal processing. I. Title. II. Series: Report of investigations (United States. Bureau of Mines) ; 8711.

TN23.U43 [TN297] 622s [622'.8] 82-600087

CONTENTS

ILLUSTRATIONS

ILLUSTRATIONS--Continued

TABLES

PERFORMANCE EVALUATION OF ELECTROMAGNETIC TECHNIQUES FOR THE LOCATION OF TRAPPED MINERS

By John Durkin [1]

ABSTRACT

The Bureau of Mines has conducted field studies in coal mines throughout the United States to determine the effectiveness of electromagnetic techniques in locating miners trapped underground following a mine accident. Data from these tests have been used to generate models of expected signal and noise distributions as found above mines throughout the coalfields. These distributions have aided in placing the expected performance of a through-the-earth electromagnetic communications technique into a probabilistic framework. Results show that at a 10-pct false alarm rate, the expected probability of detecting a miner's signal from a depth of 1,000 ft is 54 pct; at 500 ft it is 95 pct. These depths exceed the actual depths of 90 pct and 50 pct, respectively, of U.S. coal mines. Sensitivity studies have shown that at a depth of 1,000 ft, for every 3 db of improvement in signal-to-noise ratio, the probability of detection increases 6 to 8 pct.

[1]Electrical engineer, Pittsburgh Research Center, Bureau of Mines, Pittsburgh, Pa.

INTRODUCTION

Following the Farmington mine disaster in 1968, the Bureau of Mines contracted with the National Academy of Engineering (8)[2] to recommend means to increase the probability of survival and rescue of men trapped in underground mines. The Bureau considered these recommendations as the starting point for a continuing concentrated research effort to improve survival and rescue capability.

The condition of a mine after a fire or explosion is unpredictable; for example, cables may be cut and passages blocked. A hardened communication system that advances with the working face would be prohibitively expensive and might be inoperative when needed. Detection of and communication with miners trapped underground requires signaling from the surface through the mine workings or directly through the strata.

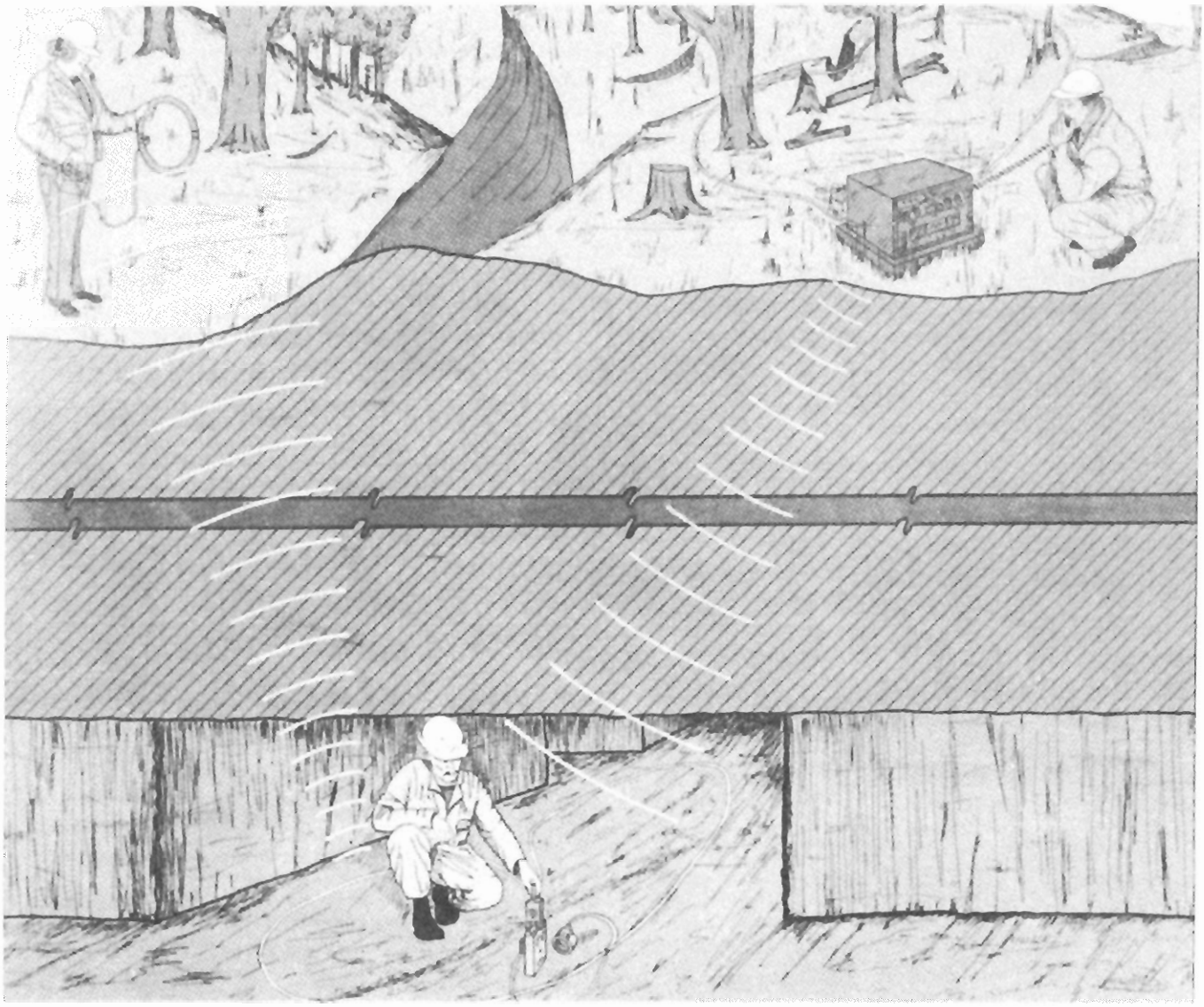

FIGURE 1. - Illustration of the operation of the trapped-miner transmitter.

[2]Underlined numbers in parentheses refer to items in the list of references at the end of this report.

The two major areas investigated in rescue communications are electromagnetic (EM) and seismic. A review of the operation and capability of seismic communications with trapped miners was published in 1981 (3). The present paper examines the potential effectiveness of the EM signaling system and is particularly concerned with the statistical analysis of experimental magnetic field strength data taken at 94 coal mine sites well distributed over the U.S. coalfields. This data-gathering venture was intended to provide the necessary information for studies of probable effectiveness of the EM signaling system prior to initiating the formulation and promulgation of new regulations bearing on the use of such a system.

During the last decade theoretical studies and field tests have indicated that the best chance of successfully rescuing trapped miners rests in a system consisting of an underground narrowband transmitter and a surface receiver, either used in a helicopter or hand-carried by surface personnel, that would both detect the signal and locate its origin. Figure 1 illustrates the principle of operation of the EM trapped-miner signaling device and associated surface receiving hardware. The transmitter and receiver were developed by Collins Radio (1).[3] An improved version has recently been built by General Instrument Corp. (GI) (5) and is shown in figure 2.

In practice, the miner would attach the belt-worn transmitter to a caplamp battery and deploy 300 ft of #18 copper wire around a coal pillar. If the loop cannot be deployed around a coal pillar, it can be deployed along a passageway where attempts are made to maximize the loop area. The transmitter delivers to the loop a pulsed square wave voltage of 630, 1,050, 1,950, or 3,030 Hz of 100-msec duration and a 10-pct duty cycle. The established EM field is then detected by surface personnel. Once the signal is detected, the surface crew deploys a large loop of wire coupled to a high-power audio amplifier that can be used for transmitting voice communications to the trapped miner. The underground transmitter contains a baseband receiver to receive the voice signals from the surface, and the miner can

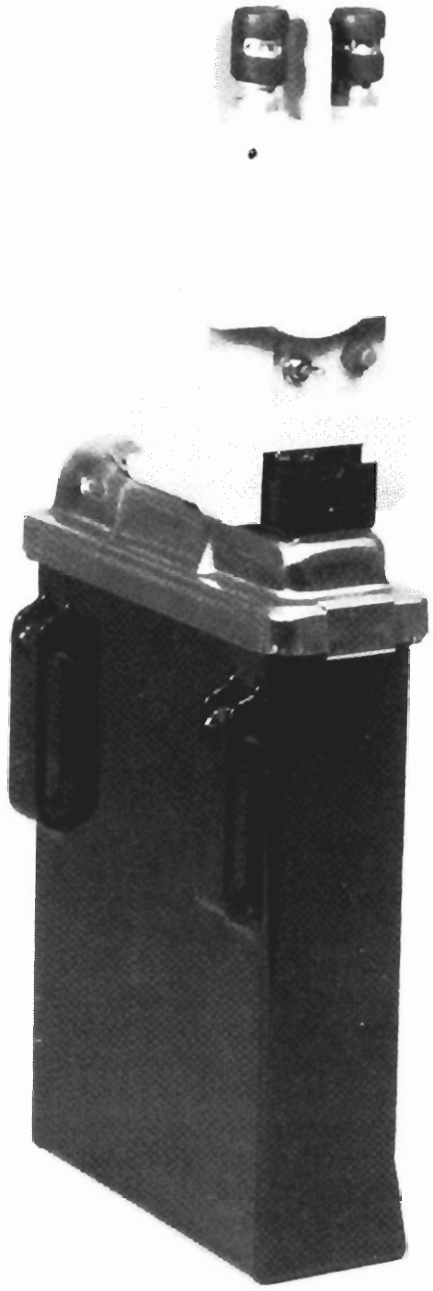

FIGURE 2. - Trapped-miner EM transmitter with caplamp battery.

[3]Use of brand names is for identification purposes only and does not imply endorsement by the Bureau of Mines.

respond in code by keying the transmitter off and on. Figure 3 shows the life expectancy of the caplamp battery when operating the transmitter. The range of values was obtained when using an old battery with an 8-hr discharge to an upper bound where a new battery with no discharge was used. A 2-ohm resistance was used as a load on the transmitter for these results. From figure 3 it can be seen that the transmitter can be expected to operate for approximately 2 to 4 days.

The objective of the field tests was twofold: First, to define a signal transmission measurement and analysis program to obtain a reliable data base for characterizing the signal transmission properties of overburdens in the U.S. coalfields; and second, to use this data base to predict the likelihood of successful performance of the EM trapped-miner signaling system. The mines sampled for these tests were selected from a population of all coal mines on the basis of both the overburden depth and for the number of miners employed at the mine. The sample reflected concern both for the physical dependence of signal penetration on depth and for the number of miners exposed to potential emergencies within each depth interval. Figure 4 shows the cumulative distribution of mines as related to the maximum depth and demonstrates that approximately 90 pct of the coal mines within the United States are less than 1,000 ft deep. These tests were performed by Westinghouse (17) and Bureau personnel. The analysis of the data as presented in this paper was performed by personnel of Arthur D. Little Inc. and the Bureau; details of this work can be found in an excellent report by Lagace (7). Numerical values of field strength and noise levels are slightly in error in the Lagace report owing to calibration errors in the antenna which were discovered later. Adjustments were made, and the data are correctly reported in this report.

EARTH TRANSMISSION LOSS

To predict the surface signal level as produced from an underground transmitter, it is necessary to understand the expected loss the signal incurs when transmitted through the earth. Unfortunately, the geological structure of the overburden above coal mines differs from mine to mine, which gives rise to differing electrical conducting properties. Therefore, for a given mine depth it can be expected that signal transmission characteristics will vary significantly from mine to mine. Consequently, one must rely on statistical information of the earth's transmission loss. A major objective of the 94-mine field test was to obtain enough data on the earth's transmission loss, as found over a large population of coal mines, to confidently characterize expected signal loss from an underground transmitter.

To insure success in obtaining these data during the field tests, magnetic moments of the underground transmitter were used that were artificially higher than would be expected from a transmitter to be used by a miner. Therefore, in most cases, an earth transmission loss value for each mine was obtained. A strategy could then be formed to predict the expected surface signal strength based upon a given magnetic moment.

The root-mean-square (RMS) values of the vertical magnetic field, H_z, of all of the data taken were normalized to a transmitter magnetic moment (M) of $M = 1$ amp-m^2. Since the surface field is directly proportional to the magnetic moment of the underground transmitter, the expected level of the surface field for a given transmitter could then be found by accounting for the actual magnetic moment used. Following this normalization, statistical studies were performed to relate the surface field strength and mine depth at each frequency tested.

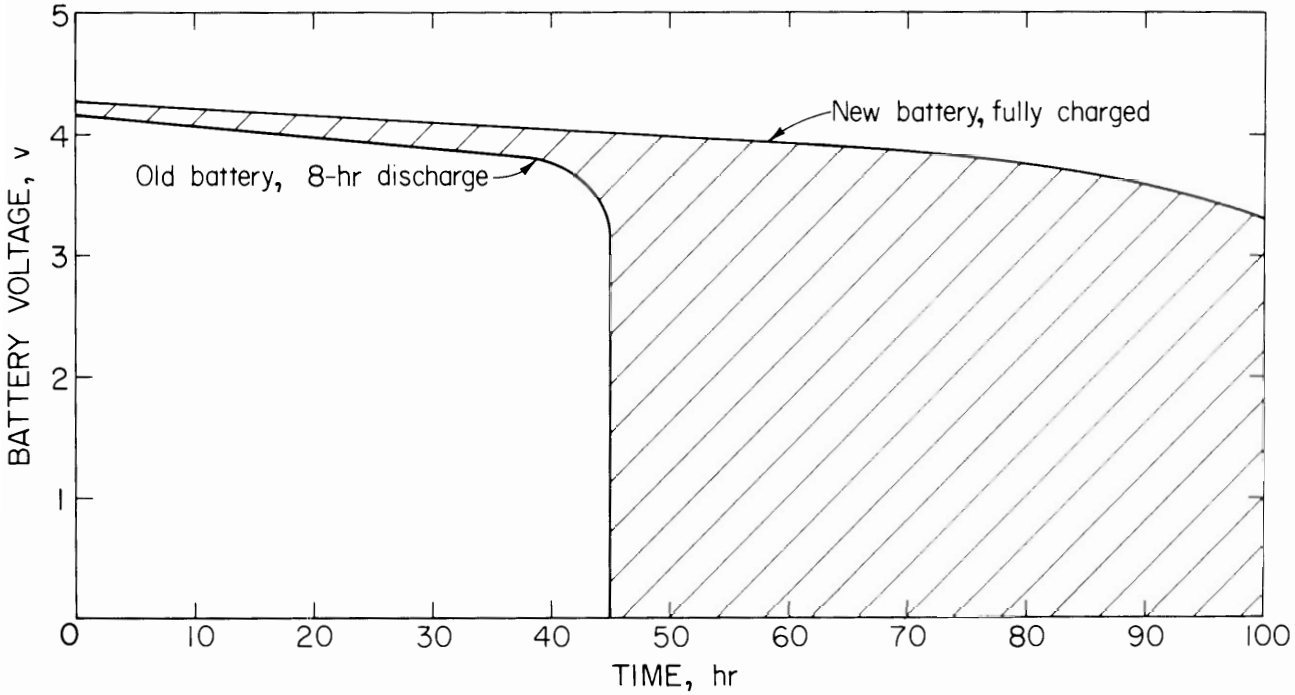

FIGURE 3. - Caplamp voltage variation with time while operating the trapped-miner transmitter.

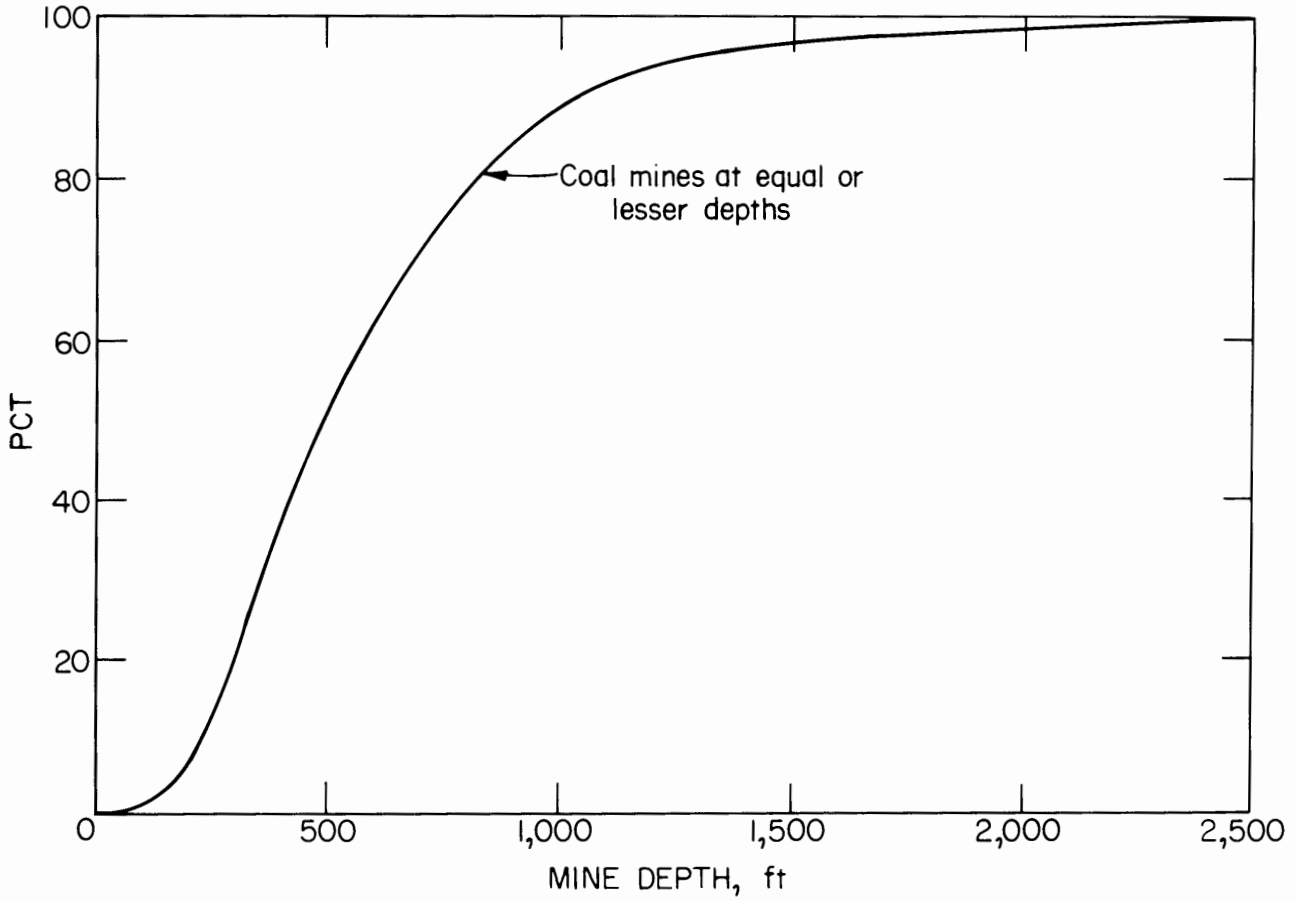

FIGURE 4. - Cumulative distribution of coal mine depths throughout the United States.

Each normalized data point can be denoted as S_{ij}, where the subscript i represents the specific frequency and the subscript j represents the specific depth of test for each mine. Thus, each surface measurement S_{ij} taken can be considered as a single observation of signal strength at a predetermined frequency and overburden depth level at a particular mine.

The relationship between field strength and mine depth was found through regression analysis. This work assumes that the errors are normally distributed and the variance is equal across the independent variable. These assumptions were considered, and it was concluded that meaningful statistical inferences from the regression analysis were acceptable.

Several linear regression models were hypothesized and tried. The model found to best fit the behavior of the data is one in which the mean value of the normalized signal strength S_{ij} is linearly related to the logarithm of overburden depth. This is shown in equation 1:

$$S_{ij} = \alpha_i + \beta_i \log (\text{depth}) + \varepsilon_{ij}. \quad (1)$$

Here S_{ij} is the normalized vertical magnetic field signal strength (expressed in decibels re 1 μamp/m-RMS for the ith frequency and depth j for a transmit magnetic moment of M = 1 amp-m^2).

The parameters α_i and β_i are to be estimated from the data, where depth is known in meters. The parameter ε_{ij} represents a random variable that is normally distributed, with expected value zero and variance σ^2_{ij}, which is the same for all values of j.

The derived regression lines for each of the four frequencies are plotted in figures 5 through 8. The R^2 statistic, a measure of goodness of fit, indicates that the log-linear relationship is appropriate.

Two types of intervals have been estimated from the data. One is known as a confidence interval, which is defined as a range of values computed from the sample that can be expected to include the true (but unknown) mean value with a known probability. Figures 9 through 12 display 95-pct confidence intervals with dashed lines. To illustrate this concept using figure 9, it follows from the field experiment that the probability is 0.95 that the interval from -8 to -14 db includes the true mean normalized signal strength for a transmitter of magnetic moment M = 1 amp-m^2 at 630 Hz and an overburden depth of 190 ft.

While the confidence interval represents a probability statement about a mean value over many trials, it is also of interest to quantify the expected outcome of a single trial. For example, what signal strength could be expected if a test were conducted at a predetermined frequency and overburden depth? This situation is depicted by prediction intervals, also plotted in figures 9 through 12. To illustrate this concept, again using figure 9, the probability is 0.95 that another test performed at 630 Hz at a depth of 500 ft would yield a signal strength between -51 and -24 db. Also plotted in figures 9 through 12, for comparison, is a curve of the free-space vertical field strength that would be measured on the surface in the absence of the lossy overburden media.

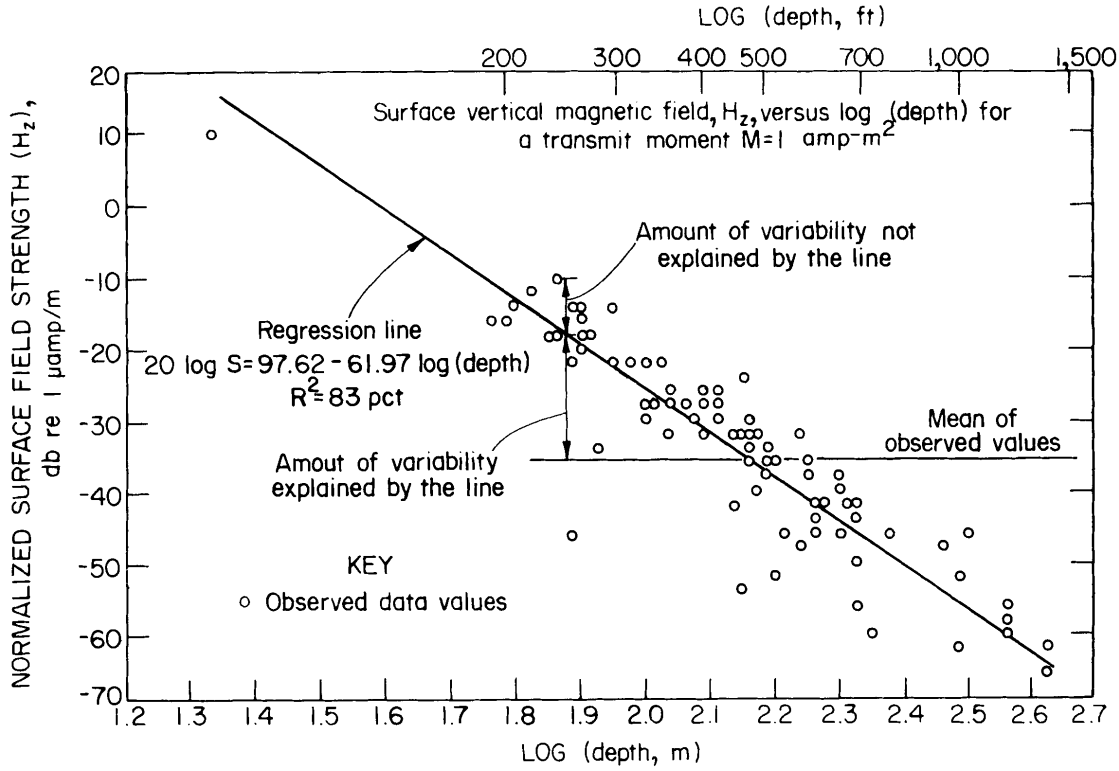

FIGURE 5. - Uplink normalized overburden signal response data and linear regression log (depth) model at 630 Hz.

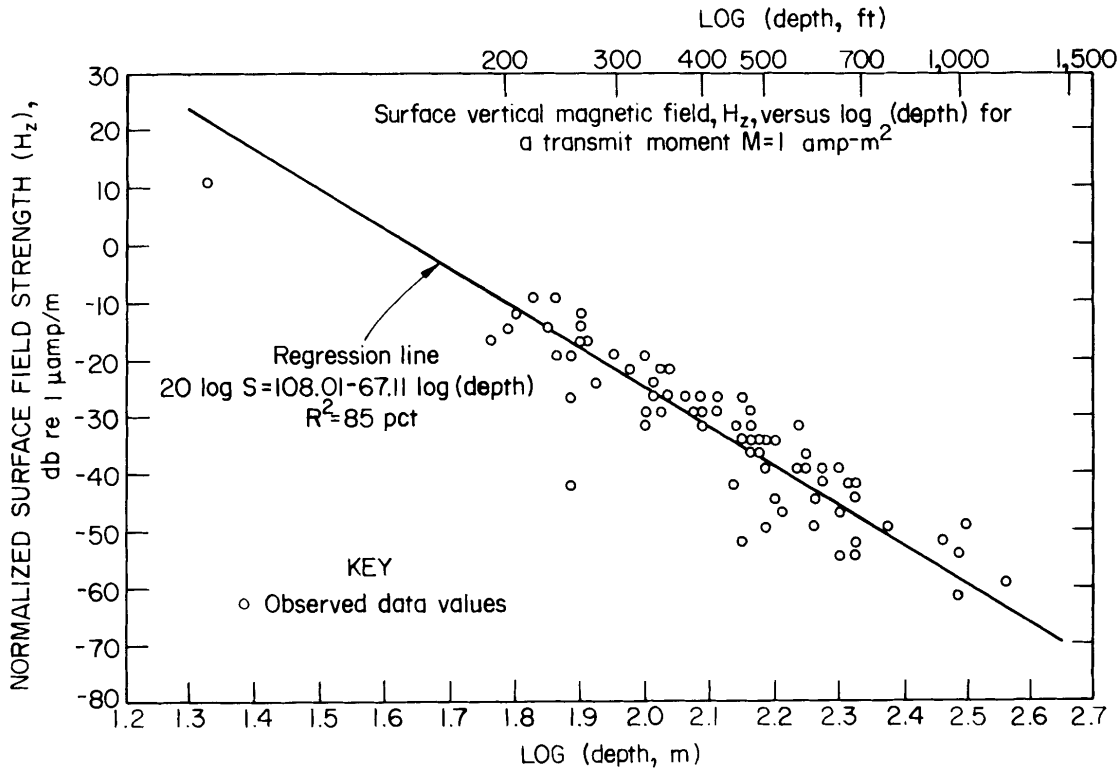

FIGURE 6. - Uplink normalized overburden signal response data and linear regression log (depth) model at 1,050 Hz.

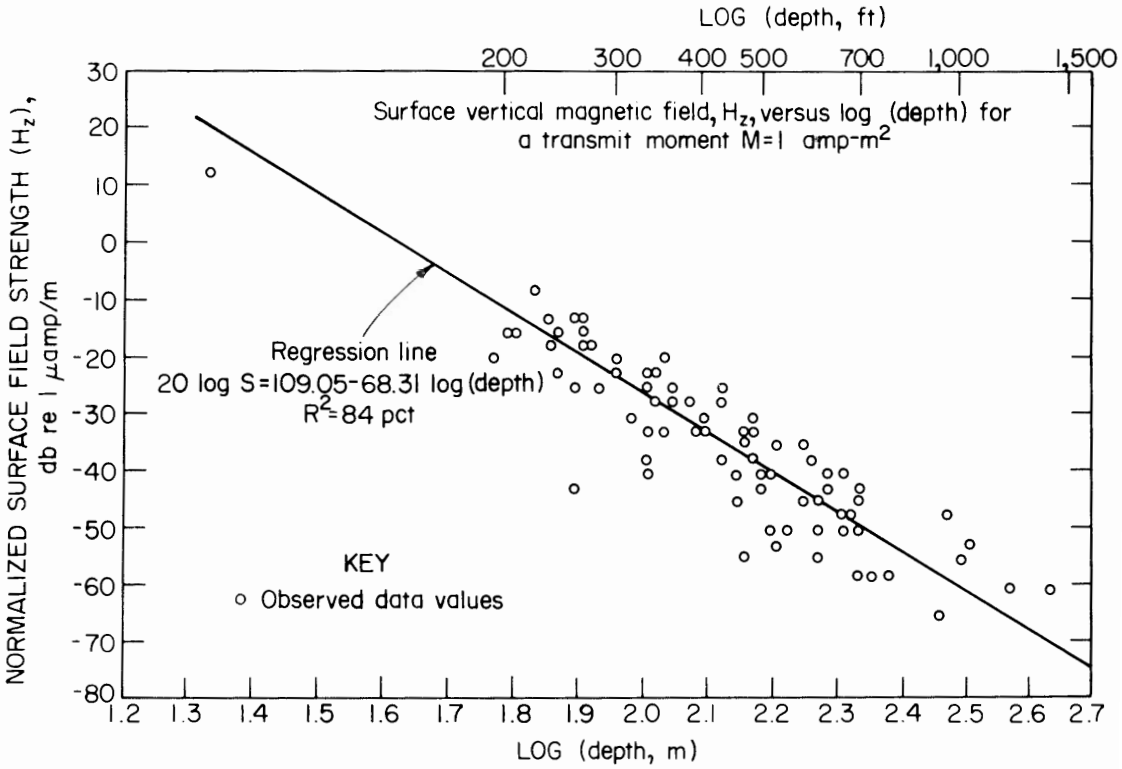

FIGURE 7. - Uplink normalized overburden signal response data and linear regression log (depth) model at 1,950 Hz.

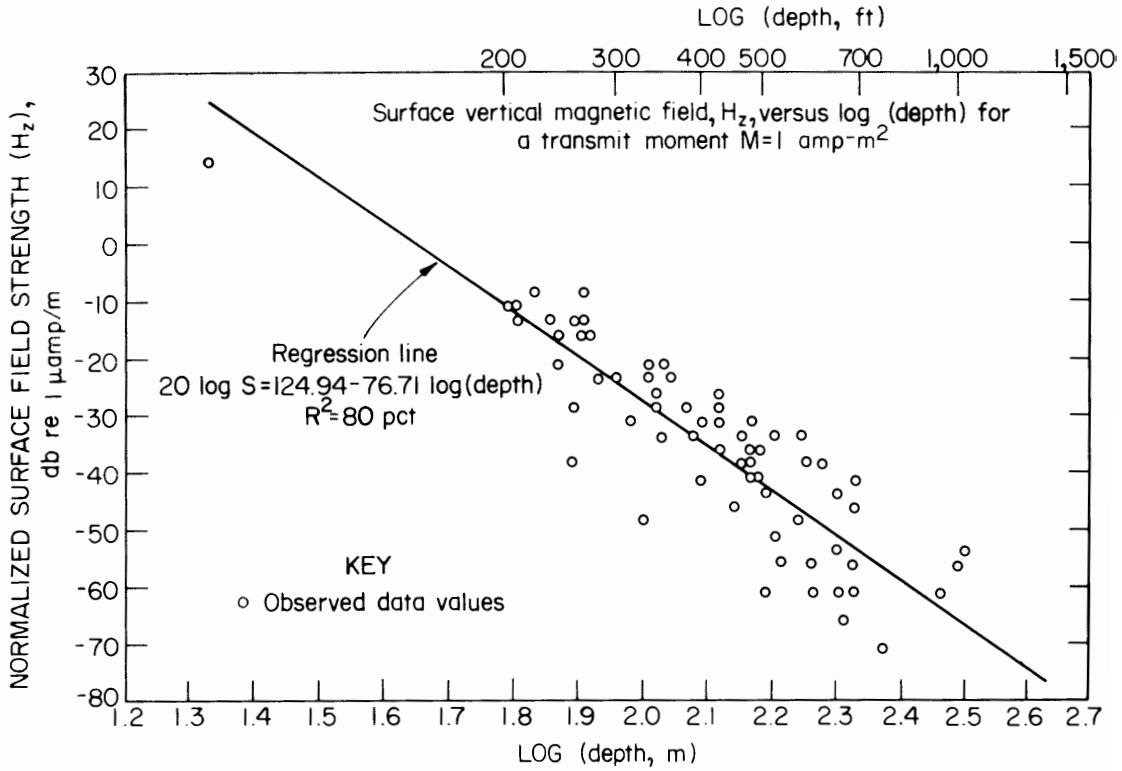

FIGURE 8. - Uplink normalized overburden signal response data and linear regression log (depth) model at 3,030 Hz.

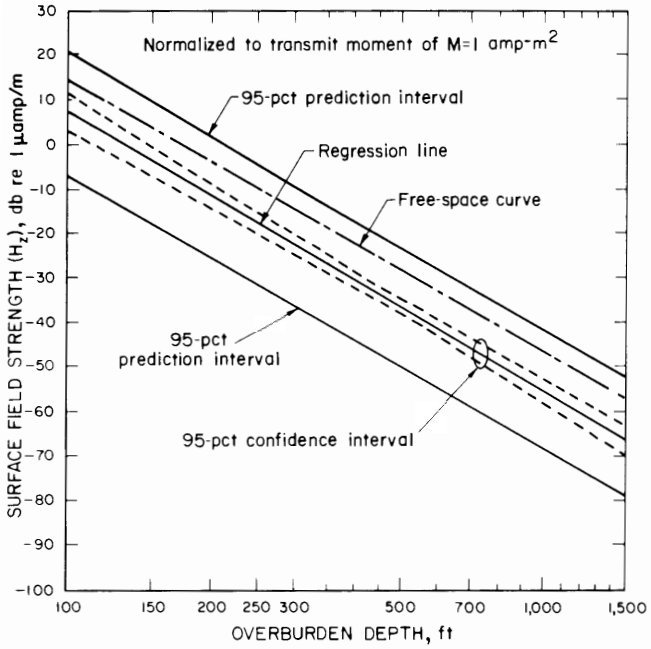

FIGURE 9. - Uplink regression results for 630-Hz-normalized vertical signal strength versus depth.

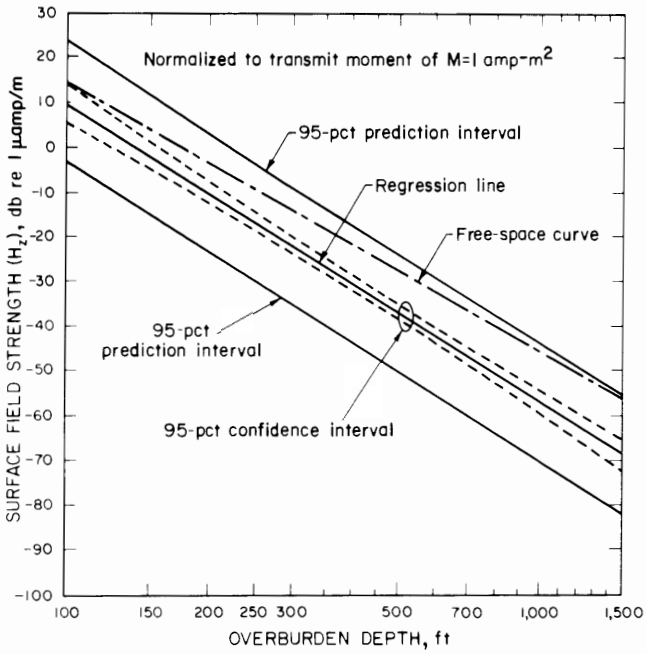

FIGURE 10. - Uplink regression results for 1,050-Hz-normalized vertical signal strength versus depth.

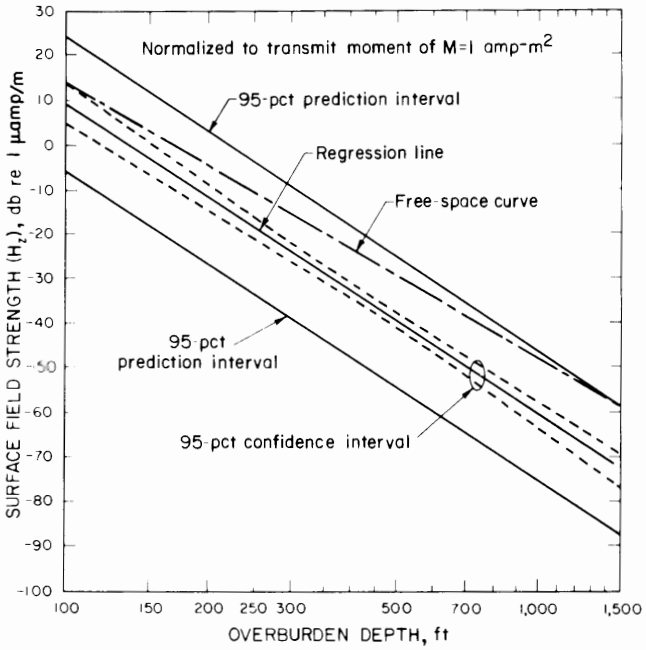

FIGURE 11. - Uplink regression results for 1,950-Hz-normalized vertical signal strength versus depth.

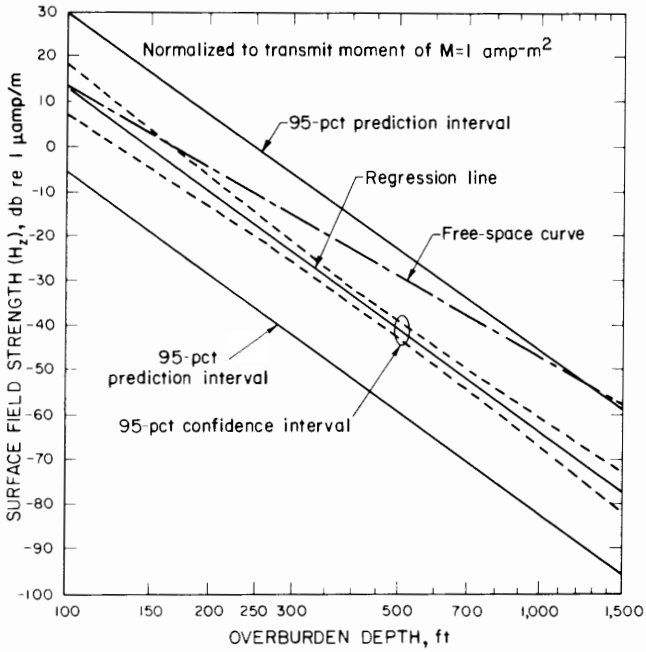

FIGURE 12. - Uplink regression results for 3,030-Hz-normalized vertical signal strength versus depth.

Figure 13 summarizes the normalized average overburden response as a function of depth and frequency by plotting the four regression lines and the free space curve on one graph. This figure shows that the frequency dependence of signal strength is relatively insignificant for depths less than 500 ft, and that the change across the band is only about 10 db even at the maximum depth of 1,500 ft.

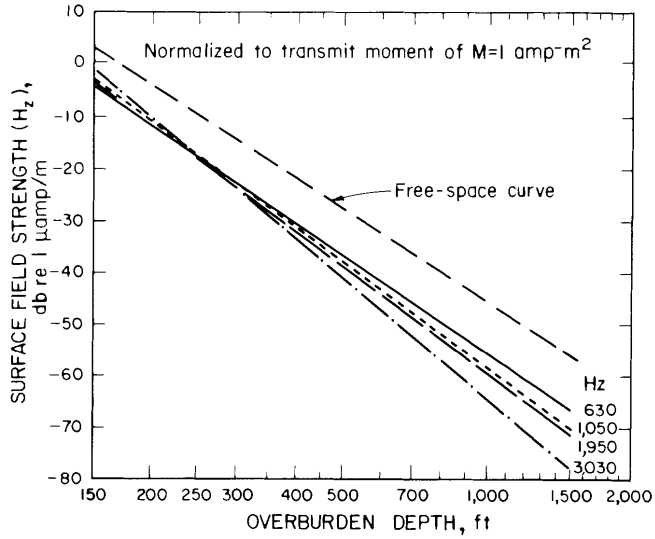

FIGURE 13. - Normalized overburden response curves—uplink regression results: Average surface vertical signal strength versus overburden depth by frequency.

These summary normalized overburden response plots, together with the confidence and prediction levels of this section, can be used to generate estimates of signal strength produced on the surface above coal mines as a function of overburden depth and operating frequency for transmitters having any prescribed magnetic moment versus frequency characteristics in the 630- to 3,030-Hz band. This assumes that, for a fixed magnetic moment, the size of the transmitting loop has no influence on the surface field. It is recognized that this assumption is not totally valid, as demonstrated by Wait (16), but it is felt that the size of loop used during the tests and the typical offsets for measuring the surface field were not severe enough to greatly influence the results.

GENERAL INSTRUMENT TRANSMITTER

Using the results of the previous section on earth transmission loss statistics, the expected surface signal strengths produced by the recently developed GI transmitter can be predicted by computing the expected magnetic moment at each frequency and then translating each of the overburden response curves of figure 13 upwards by an amount equal to the values of the magnetic moment expressed in re 1 amp-m^2.

The GI loop antenna consists of 300 ft of #18 copper wire, arranged in a square. This loop configuration was chosen because it best represents the practical implementation of the strategy that the miners will be instructed to follow. Figure 14 shows the predicted surface field strength when the GI transmitter is used. Also shown are the expected magnetic moments for each frequency.

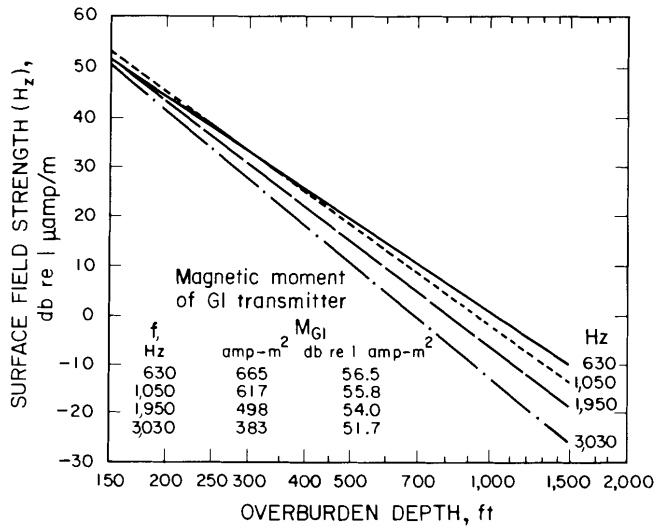

FIGURE 14. - Predicted uplink response curves for General Instruments transmitter: Average surface vertical magnetic field signal strength versus depth by frequency.

SURFACE EM NOISE

Two independent sets of magnetic field noise measurements were obtained during the measurement program. The first was by Westinghouse using the Collins man-carried receiver. This set of data was found to be in error owing to intramodulation problems caused by the simultaneous measurement of discrete manmade noise and broadband noise. The second set of data was obtained by a Bureau team performing tests at 27 of the mines tested. The Bureau's data were gathered on tape and later analyzed in the laboratory.

For purposes of signal detectability, the RMS value of the vertical magnetic field is of interest. The statistical distribution of this noise, using the Bureau data base, at each frequency for a receiver bandwidth of 30 Hz is shown in figures 15 through 18.

SURFACE SIGNAL-TO-NOISE RATIO

In the previous sections, the behavior of signal data and noise data obtained in this study has been characterized by statistical relationships. It has been found that both the signal and noise data are log normally distributed. To develop an understanding of detection probability, it is necessary to characterize the probability distributions of the surface RMS signal-to-noise ratio (SNR) at each frequency.

The basic input for the derivation of RMS-SNR estimates on the surface is summarized in table 1. Mean RMS signal strength and standard deviation values at each frequency for different mine depths are given, adjusted to pertain to the GI transmitter. Mean RMS noise strengths and their standard deviations are also given at each frequency.

TABLE 1. - Estimated parameters characterizing signal and noise distributions above coal mines

Overburden depth, ft	630 Hz	1,050 Hz	1,950 Hz	3,030 Hz
ESTIMATED MEAN SIGNAL IN DECIBELS RE 1 μamp/m FOR GI TRANSMITTER				
250.....	37.50	37.51	34.50	32.27
500.....	18.84	17.31	13.93	9.18
1,000.....	.19	-2.90	-6.63	-13.92
1,500.....	-10.72	-14.71	-18.66	-27.42
Standard deviation.....	6.65	6.52	7.08	8.92
ESTIMATED MEAN NOISE IN DECIBELS RE 1 μamp/m / $\sqrt{30}$ Hz				
All depths.....	4.3	-2.8	-11.3	-17.1
Standard deviation.....	13.5	11.5	12.5	12.5

The independence of signal and noise distributions, in addition to the property of normality exhibited by each distribution, permits straight-forward combination of the two distributions to generate SNR probability estimates. The sum (or difference) of two normally and independently distributed variables is also normally distributed.

The SNR distributions are conveniently plotted using normal probability paper. This paper is designed so that the mean is plotted at the 50 percentile point and the mean plus and minus one standard deviations are plotted at the 16 and 84 percentile points, respectively. Such normal probability plots are given in figures 19 through 22 for five different overburden depths at each of the four frequencies.

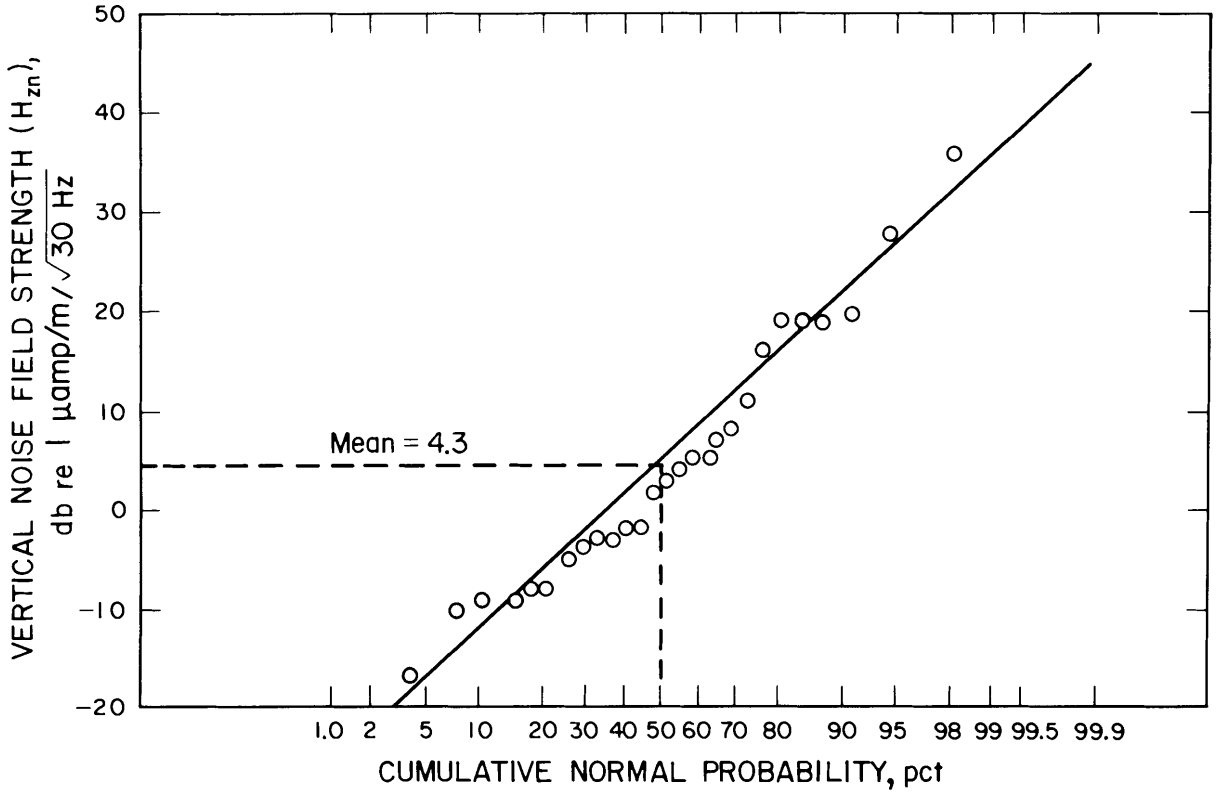

FIGURE 15. - Statistical distribution of RMS surface noise at 630 Hz.

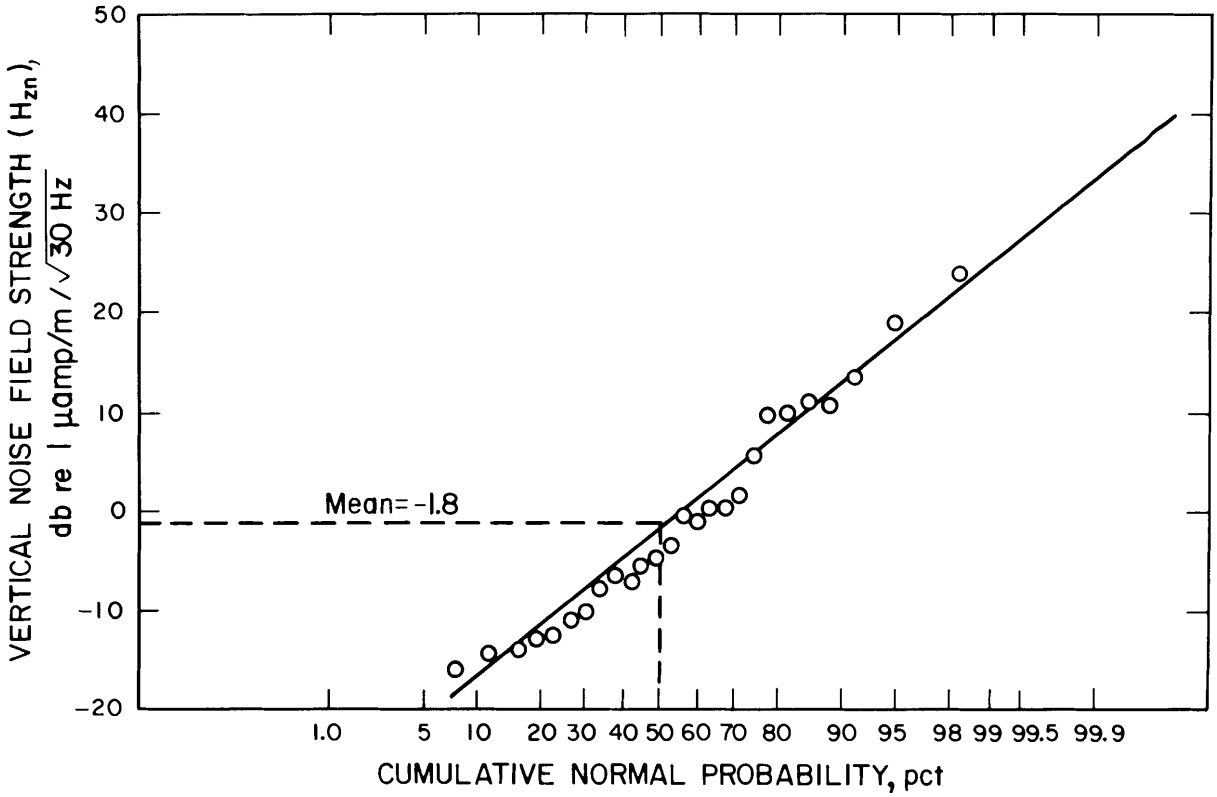

FIGURE 16. - Statistical distribution of RMS surface noise at 1,050 Hz.

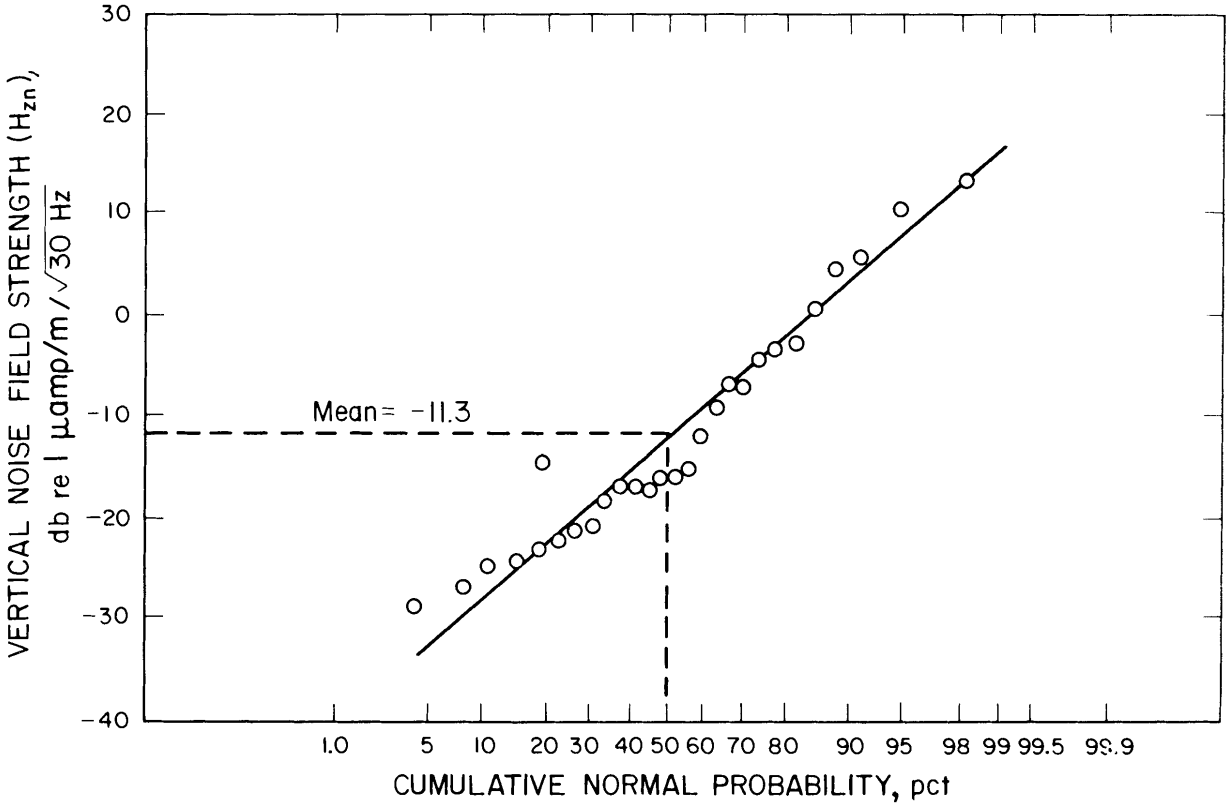

FIGURE 17. - Statistical distribution of RMS surface noise at 1,950 Hz.

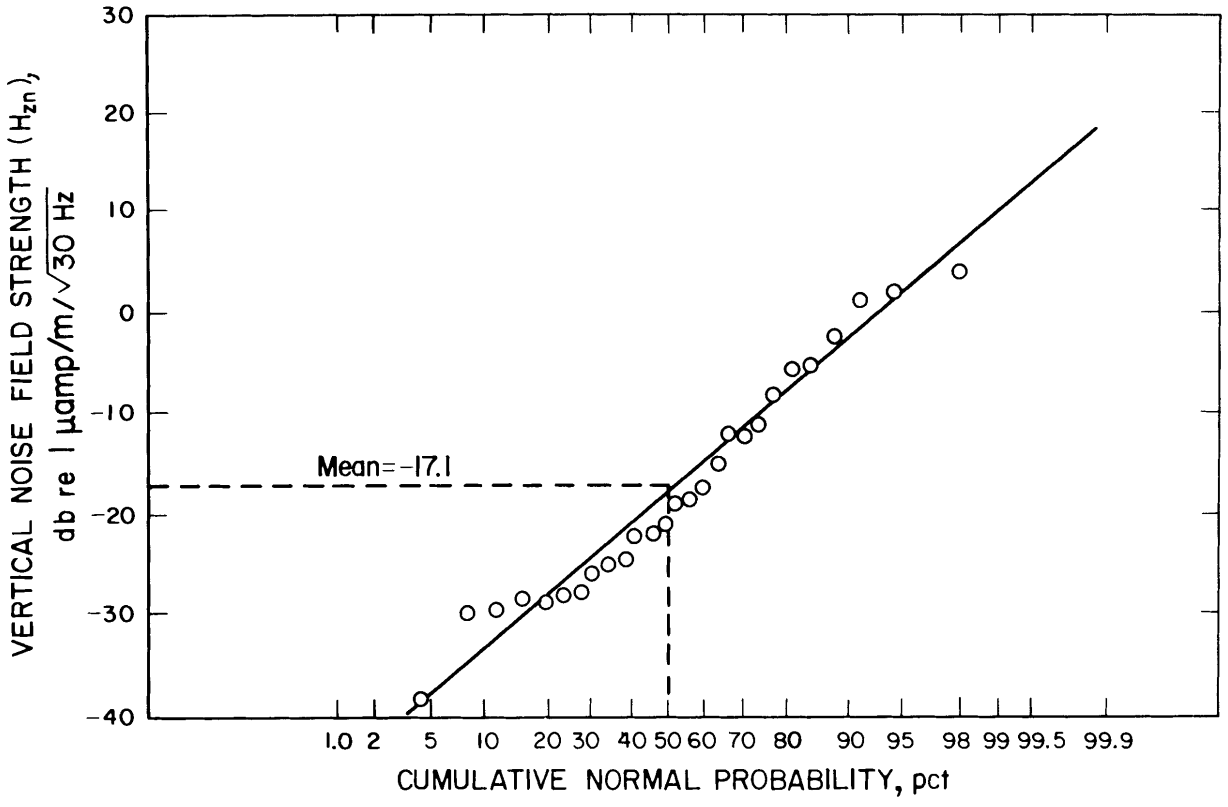

FIGURE 18. - Statistical distribution of RMS surface noise at 3,030 Hz.

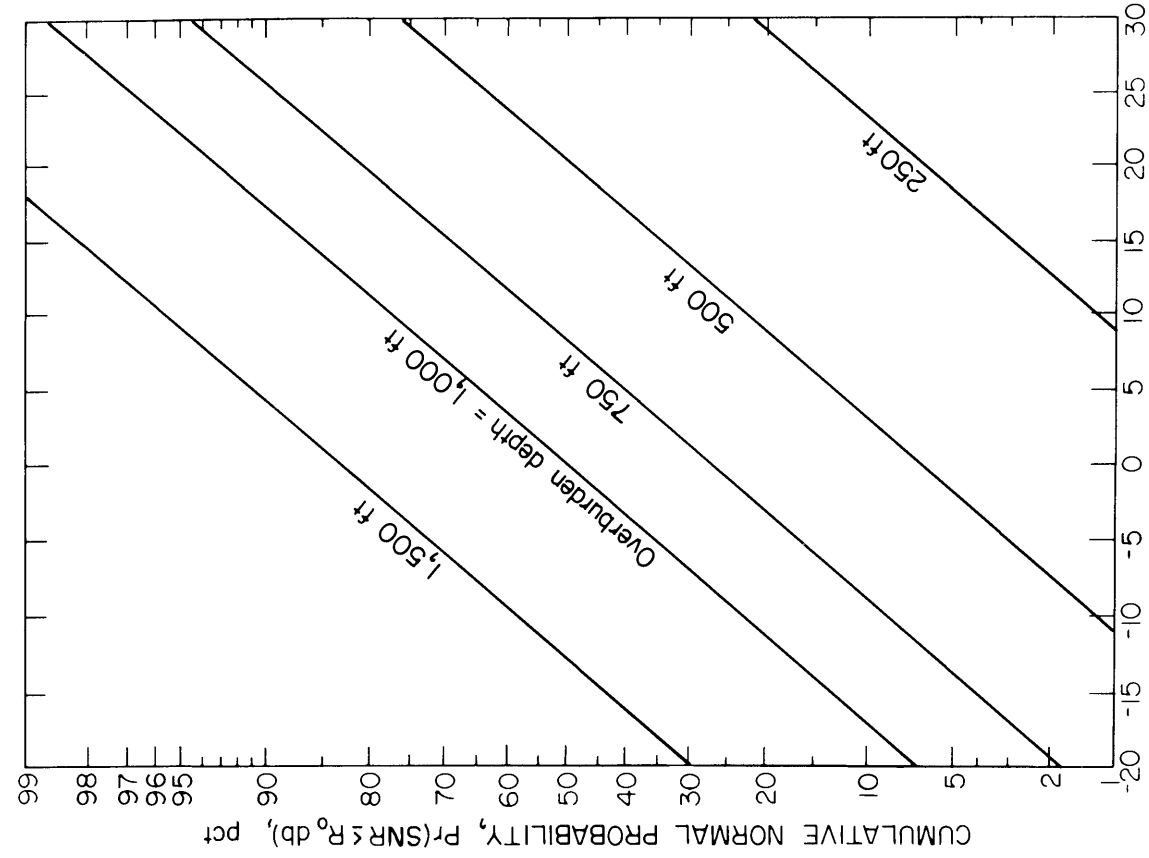

FIGURE 19. - Cumulative probability distribution of SNR expected above U.S. underground coal mines at 630 Hz.

FIGURE 20. - Cumulative probability distribution of SNR expected above U.S. underground coal mines at 1,050 Hz.

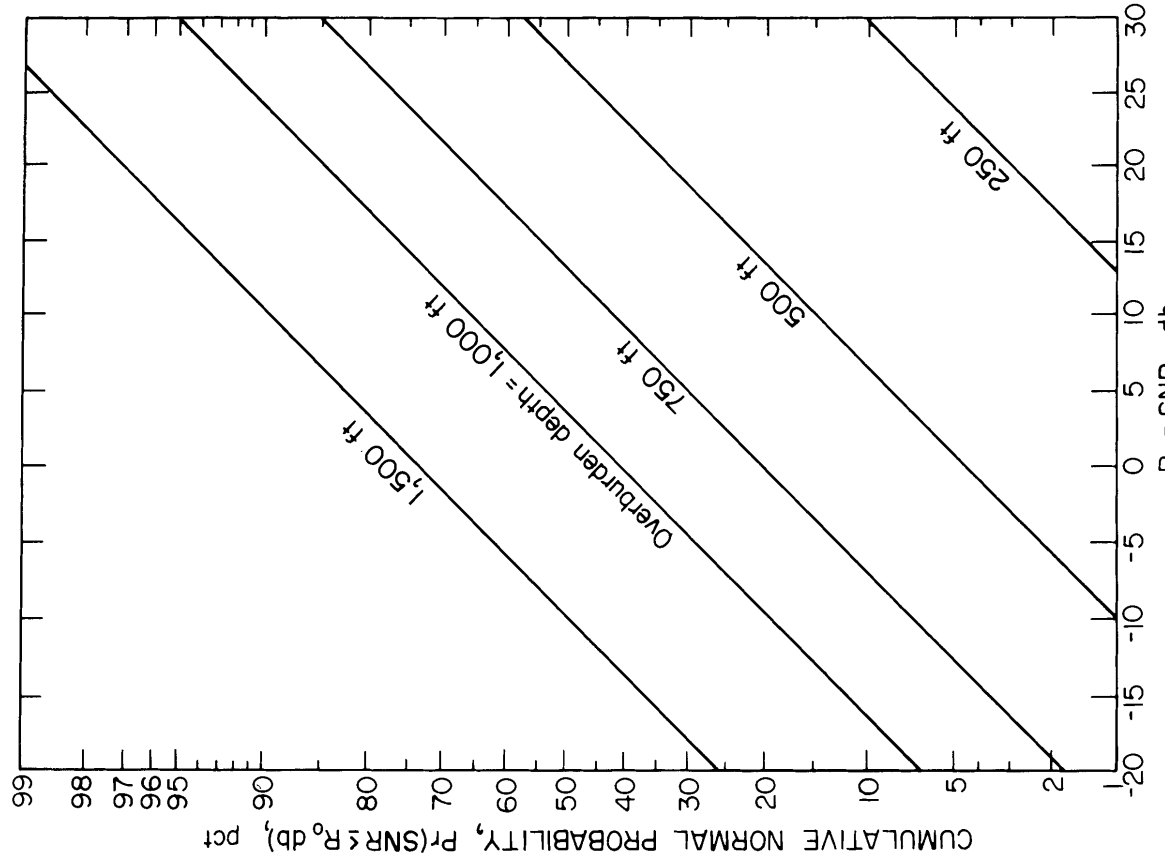

FIGURE 21. - Cumulative probability distribution of SNR expected above U.S. underground coal mines at 1,950 Hz.

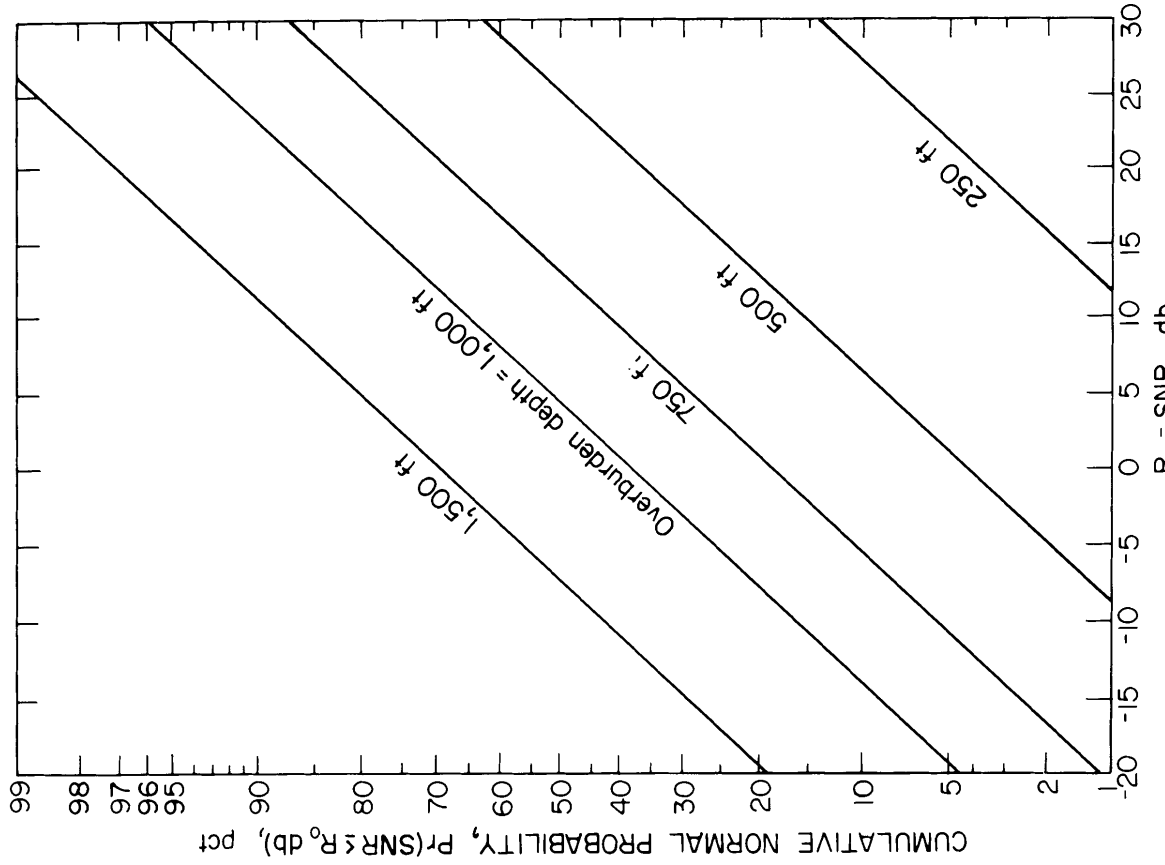

FIGURE 22. - Cumulative probability distribution of SNR expected above U.S. underground coal mines at 3,030 Hz.

These four figures provide a straightforward method to estimate the probability of having various SNR's in actual practice. The vertical axis represents the area under the normal curve from minus infinity to some SNR value R_o and provides the probability of achieving an SNR value less than or equal to R_o. Table 2 shows the probability of achieving an SNR of interest for each frequency at different depths.

TABLE 2. - Probability of achieving a signal-to-noise ratio of interest above coal mines using General Instrument transmitters

Signal-to-noise ratio, db	250 ft	500 ft	1,000 ft	1,500 ft
630 Hz				
Less than -3	0.0057	0.1101	0.5306	0.7993
-3 to 0	.0045	.0446	.0821	.0535
0 to 3	.0072	.0552	.0773	.0430
3 to 6	.0113	.0653	.0697	.0331
6 to 9	.0167	.0740	.0602	.0243
9 to 12	.0238	.0802	.0497	.0172
Above 12	.9308	.5707	.1304	.0296
1,050 Hz				
Less than -3	0.0003	0.0346	0.4109	0.7595
-3 to 0	.0004	.0224	.0935	.0671
0 to 3	.0009	.0324	.0933	.0538
3 to 6	.0018	.0445	.0880	.0408
6 to 9	.0034	.0577	.0785	.0293
9 to 12	.0061	.0709	.0663	.0198
Above 12	.9870	.7375	.1695	.0296
1,950 Hz				
Less than -3	0.0002	0.0190	0.2868	0.6263
-3 to 0	.0002	.0129	.0793	.0600
0 to 3	.0004	.0193	.0855	.0710
3 to 6	.0009	.0277	.0878	.0601
6 to 9	.0017	.0377	.0859	.0484
9 to 12	.0031	.0490	.0801	.0371
Above 12	.9935	.8344	.2944	.0770
3,030 Hz				
Less than -3	0.0001	0.0189	0.3314	0.6994
-3 to 0	.0001	.0123	.0804	.0697
0 to 3	.0003	.0182	.0843	.0596
3 to 6	.0005	.0259	.0845	.0487
6 to 9	.0010	.0351	.0809	.0381
9 to 12	.0019	.0455	.0740	.0284
Above 12	.9960	.8441	.2646	.0561

It is instructive to observe the behavior of probability estimates associated with exceeding a given SNR as a function of overburden depth and frequency. Figure 23 gives the probability of the RMS signal being at least greater than the RMS noise. Note that the best performance occurs in the upper part of the frequency band even though more loss occurs through the earth at the higher frequencies. This can be explained by the rapid decrease in surface noise level as frequency increases.

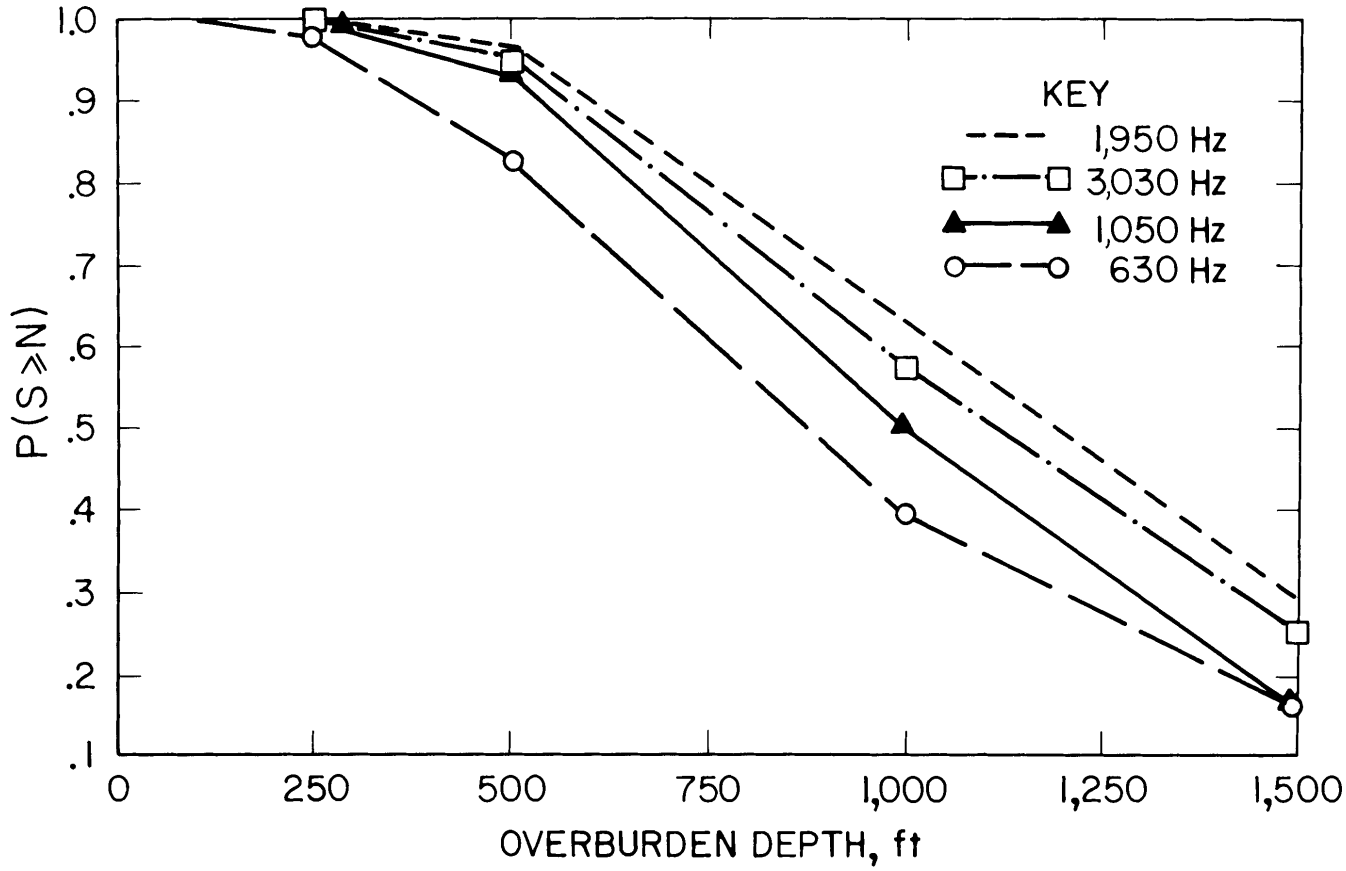

FIGURE 23. - Probability that mean RMS signal is greater than or equal to RMS noise for the General Instruments transmitter.

SIGNAL DETECTION CRITERIA

Recognition Differential Method

The success of a rescue effort when using a trapped-miner transmitter rests on the ability of surface personnel to confidently detect the signal from the underground transmitter. The pulsed signals from the underground transmitters are detected by searchers carrying rescue receivers equipped with a handheld loop antenna and headsets. The mode of detection is aural, based on the headset signals perceived by the ear. It is then necessary to establish a relationship between the nature of the signal, SNR, and the probability of aural signal detection.

The aspects of the signal that influence detection are (a) frequency, (b) signal length, and (c) signal repetition. The primary aspect of the noise for detection considerations, besides its level, is its bandwidth. How each of these parameters affects the signal detection capability must be understood; then their results can be combined to generate a probability-of-detection curve as a function of SNR.

The present receiver mixes the received signal with an internal oscillator to a higher frequency for purposes of narrowband filtering, and then mixes the filtered signal again to present a listening signal of 978 Hz to the operator. The ability to detect a tone masked by broadband noise as a function of frequency has been studied by Urick (15). In this work, an entity known as critical bandwidth evolved. When the ear listens for a tone, it acts as a narrowband filter centered at the signal frequency. The masking of the signal by the noise will

only be influenced by the noise within this critical band. Noise outside this band will have no influence on signal detectability. Figure 24 illustrates the critical bandwidth values as a function of frequency and shows that critical bandwidth is approximately 60 Hz at the 978-Hz listening frequency of the rescue receivers (15).

The effect of the length of a pulsed tone is shown in figure 25. Psychoacoustic data taken by a number of investigators are combined in this figure to show the "recognition differential" required versus pulse length for a 50-pct probability of detection (15). The recognition differential is the amount in decibels by which the signal level needs to exceed the measured noise spectrum level (noise level in 1 Hz within critical band of interest) to provide a 50-pct probability of detection.

The GI transmitters have a fixed pulse duration of 100 msec, which prescribes a recognition differential of 23 db to achieve a 50-pct probability of detection. To determine the significance of the 23-db recognition differential in terms of required SNR, a bandwidth must be chosen. The bandwidth used in the receiver is 30 Hz, one-half of the critical bandwidth of the ear at the listening frequency. It is assumed here that the noise reaching the operator's ear is produced solely by the receiver and that the attenuation provided by the headset is sufficient to justify disregarding ambient acoustic noise in the area of the operator. Studies (10) have shown that systems with bandwidths approximately one-half the critical bandwidth will behave in the same manner detection-wise as those having a system bandwidth equal to the critical bandwidth. Therefore, for purposes of the trapped-miner system, an SNR of 23-10 log 30 = 8 db is needed to yield a 50-pct probability of detection.

A final factor affecting detection is the signal repetition rate. Garner (4) provides data on the effect of the repetition of a pulsed tone on signal detectability. Figure 26 illustrates these findings. This work shows that as the repetition rate of a 50-msec pulse of a 1,000-Hz signal is changed from 1 per 4 sec to 1 per sec, 2 db less SNR is required. Reviewing Garner's data would indicate that an even greater improvement might be expected for the trapped-miner transmitter, but the lack of data at repetition rates less than 1 per 4 sec precludes a guarantee of this. Therefore, a conservative 2-db improvement value will be used. The 50-pct probability of detection SNR criterion of (8-2) db, or 6 db, will be used.

This work quantifies the necessary SNR to establish a 50-pct detection probability. It is also necessary to extend this work to determine detection probabilities at any other SNR. The results of this extension are shown in figure 27 and table 3. This plot can be used with the earlier established expected SNR for the underground GI transmitter to establish signal detection probabilities.

TABLE 3. - Probability of signal detection by observer versus signal-to-noise ratio for the recognition differential method

Signal-to-noise ratio, db	Probability of detection	Signal-to-noise ratio, db	Probability of detection
2	0.00	7	.78
3	.02	8	.90
4	.10	9	.98
5	.22	10	1.00
6	.50		

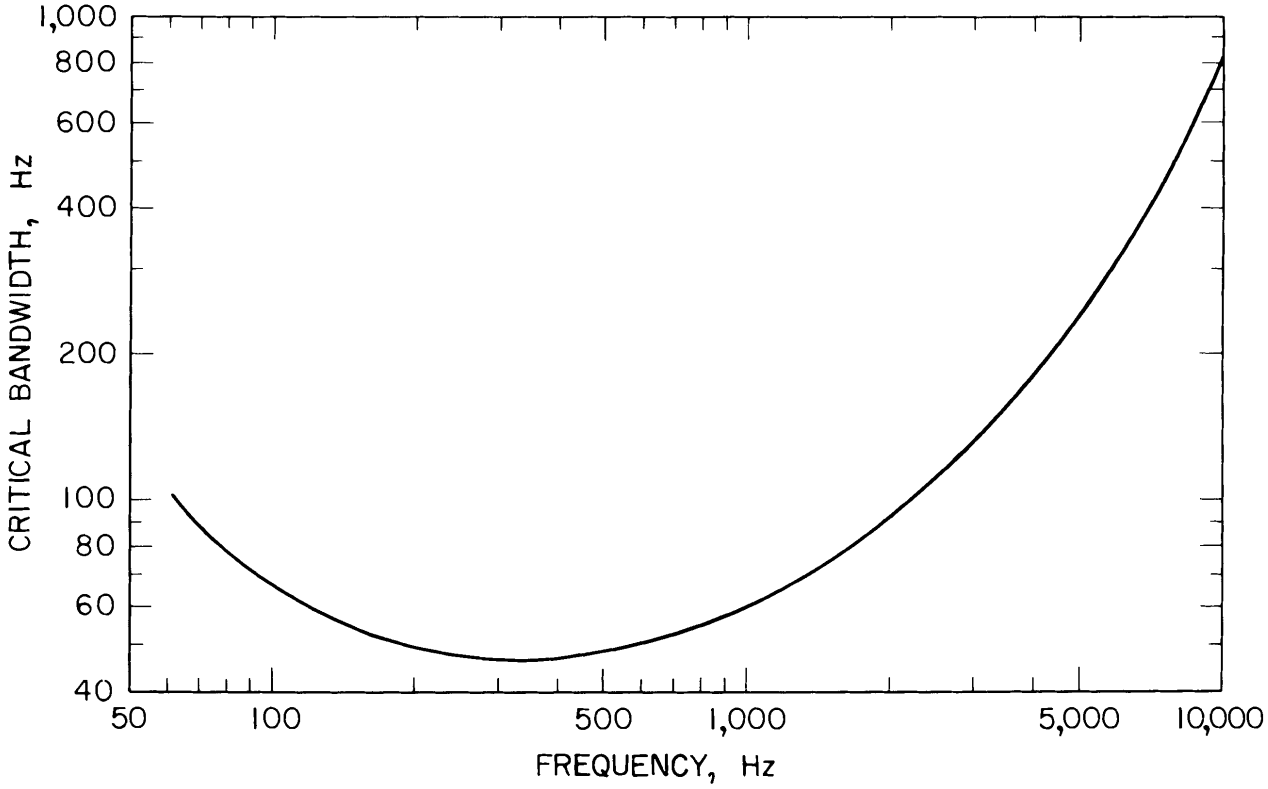

FIGURE 24. - Measured values of the critical bandwidth of the ear.

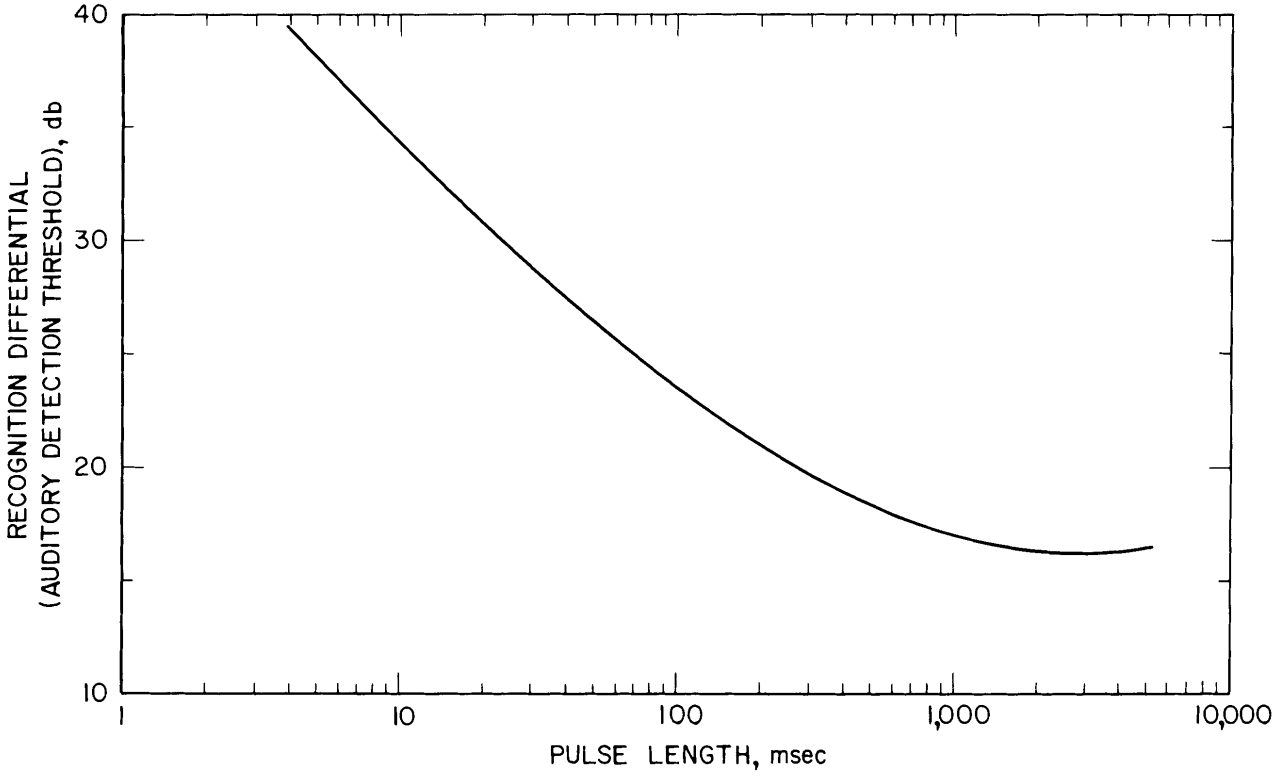

FIGURE 25. - Recognition differential (auditory detection threshold) for sinusoidal pulses in broadband noise reduced to 1-Hz bands.

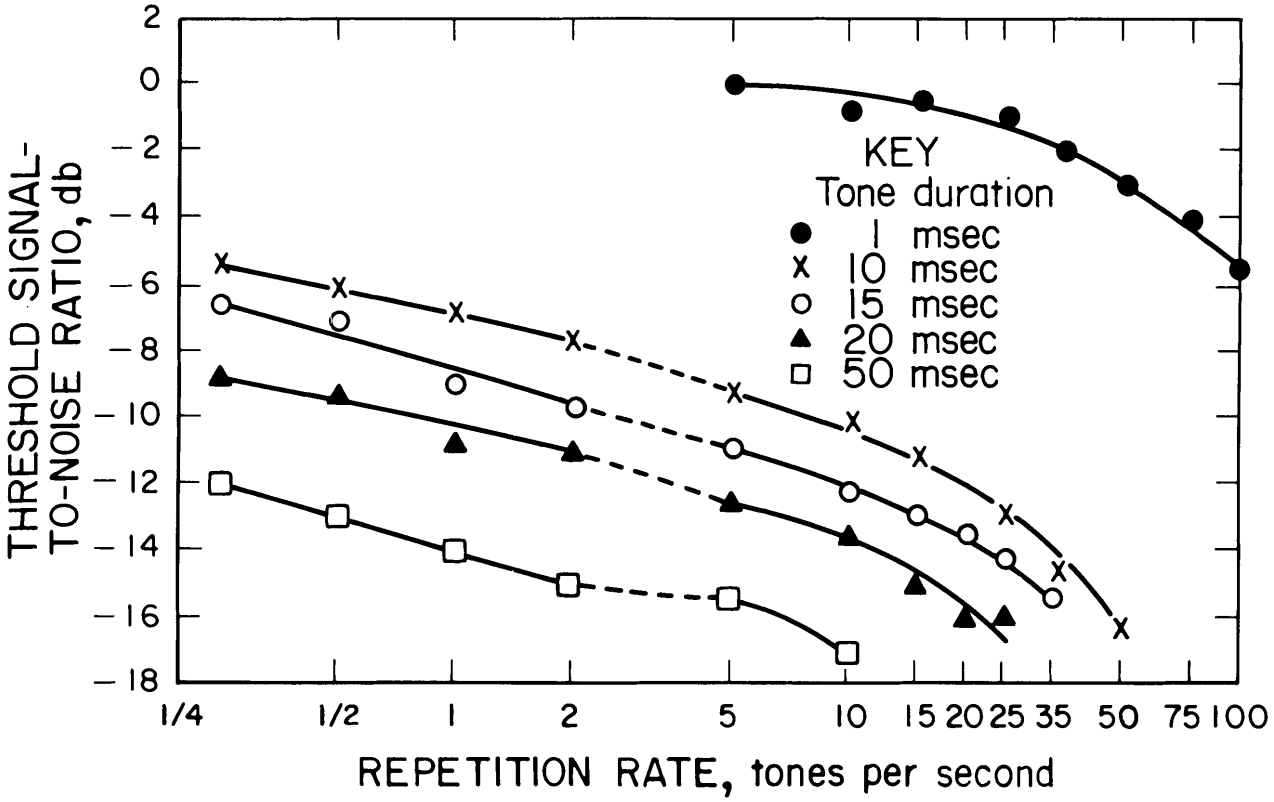

FIGURE 26. - Effect of repetition rate of short tones on the masked threshold.

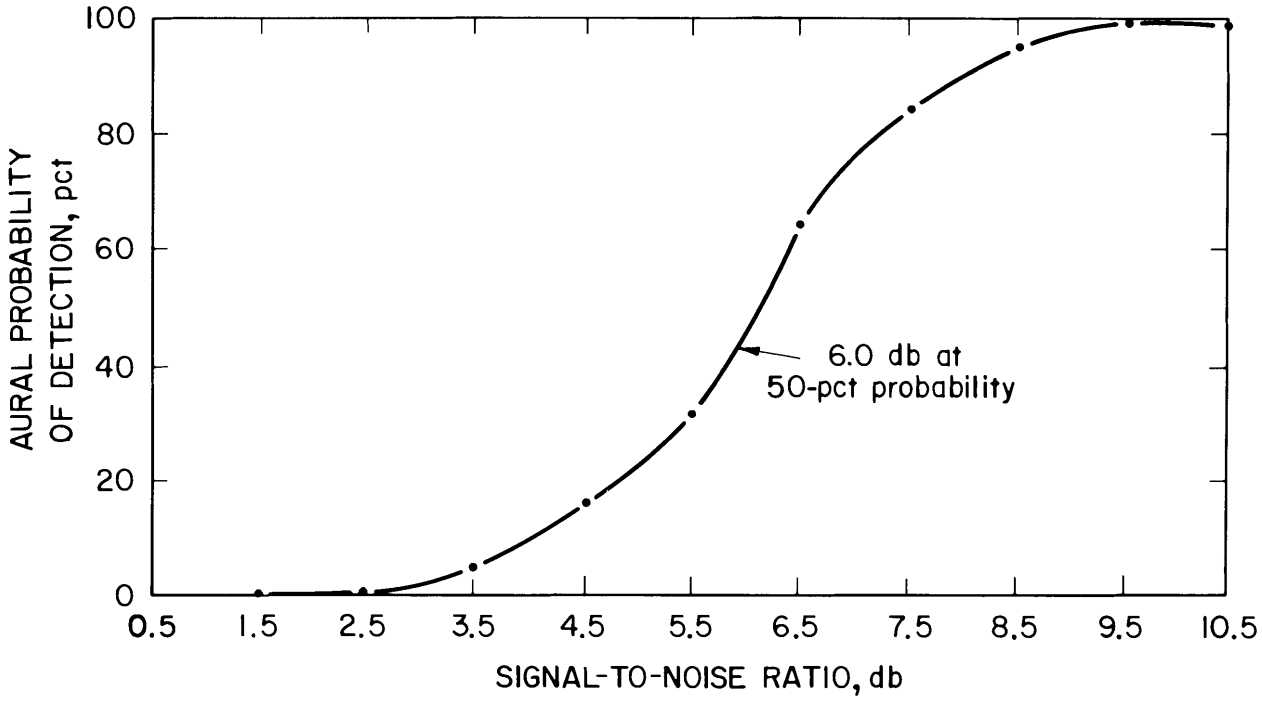

FIGURE 27. - Aural probability of detection versus RMS signal-to-noise ratio for trapped miner pulsed with the signals in Gaussian background noise.

Receiver Operating Characteristic Method

The recognition differential, as discussed in the previous section, may provide misleading conclusions since the percentage of correctly identified signals is given unaccompanied by information about either false alarms or correct rejections. This problem occurs because assumptions made about an observer's performance are not necessarily correct. If the observer is told to be certain that a signal is present, then the curve of figure 27 would be shifted to the right and the recognition differential would be higher. If, however, the observer is told to be very sure not to miss any signals, then the curve of figure 27 would be shifted to the left. In the first case, the observer misses the signal more often; in the second case, the observer produces more false alarms. Ideally it would be desirable to have a criterion-free measure in order to make meaningful statements about an observer's performance in signal detection.

Fortunately, this criterion-free measure can be obtained from earlier work by Peterson (10) on the theory of signal detectability (TSD). This work relates statistical decision theory to the general detection problem. The theory was originally developed to describe mathematically ideal or optimal detection processes, but it has become apparent that it represents a good approximation to a descriptive theory of human detection and recognition behavior (13).

The fundamental detection problem of TSD defines two parameters, the index of detectability (d') and the threshold criterion (c), which when combined provide a useful measure of performance. To understand the concept of these two parameters, refer to figure 28. Plotted in this figure are the probability density functions for noise alone (N) and for signal plus noise (SN). The mean of the N distribution has been placed at zero so that d' is read directly as the position along the abscissa of the mean of the SN distribution.

The distance between the means may be regarded as a measure of the observer's sensitivity. It is a measure of the difference in sensory response to noise and signal plus noise stimuli and is analogous to SNR. However, despite this close analogy, it is impossible to assign definite values of SNR to d'. The value c as shown in figure 28 is analogous to a threshold, and in the case for d', no definite value can be assigned to it.

To obtain a measure of d' and c and of the effectiveness of the test system, an experiment is performed in which an observer is provided a series of observation periods. At the end of each period, the observer reports his or her observation as noise only, or as signal plus noise. To accomplish this task, the observer establishes a criterion, represented by c of figure 28, and responds "no" when a particular observation is less than c and "yes" when it is greater.

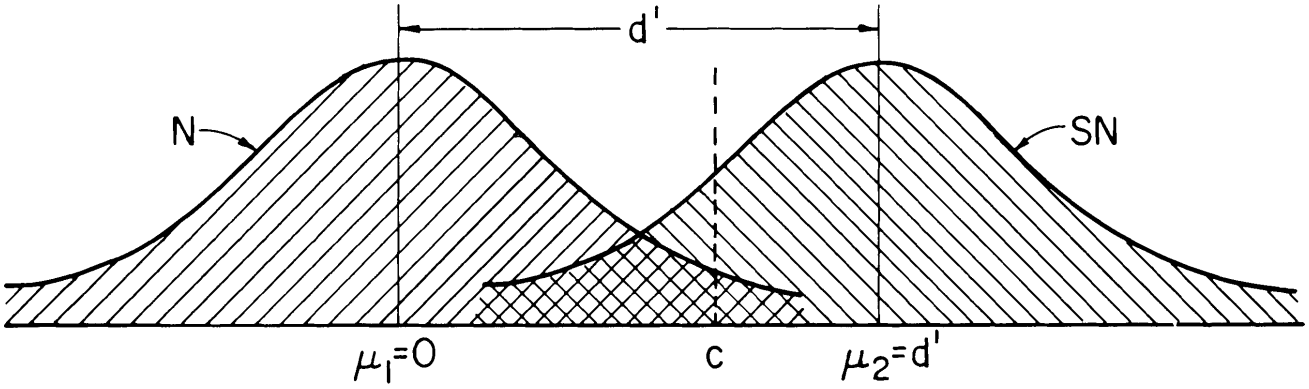

FIGURE 28. - N and SN distributions showing d' and c relationships.

Of the two parameters of interest, d' is fixed by the experimental conditions and defines the limitation imposed on the observer by the characteristics of N and SN, and by his or her own sensitivity to these characteristics. The observer to some degree controls c, but this control is to a large extent dictated by the physiological framework of the test.

In a typical test, as discussed earlier, the observer may be given such instructions at the start of the test as "Don't miss any signals," or "Be very sure you have a signal when you say yes." What it is necessary to do then is to structure the test properly in order to obtain results that will both demonstrate the observer's ability to accurately detect the signal and provide a measure of the false alarm rate. A form that provides this desired result is commonly known as the receiver operating characteristic (ROC) curve and is illustrated in figure 29.

The ROC curve can be generated directly from the N and SN distributions of figure 28. The area under the N distribution to the right of c represents the probability of false alarm, P(Y|N). The area under the SN distribution to the right of c represents the probability of detection, P(Y|SN). Each possible value of c generates a pair of values that may be mapped as a point in the P(Y|SN)-P(Y|N) plane as shown in figure 29. The d' parameter value is the distance along the negative diagonal between the ROC curve and the chance line. Thus, a set of values of d' defines a family of ROC curves.

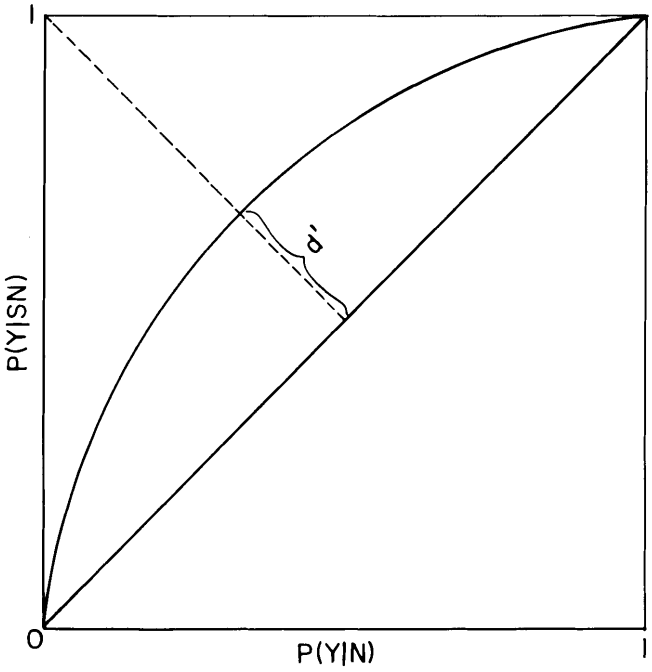

FIGURE 29. - Receiver operating characteristic curve.

In practice, the simplest way to obtain the d' value is to present to the observer a series of tests in which a signal may or may not be present on each test. From these tests, results are obtained on the probability of correctly identifying a signal, P(Y|SN); probability of false alarm, P(Y|N); probability of a miss, P(N|SN); and probability of a correct rejection, P(N|N). These values may then be used to enter a table of areas under a unit area normal distribution to obtain d'. However, this yields only one point on an operating characteristic on the negative diagonal. Since the whole ROC curve provides important additional information, it is desirable to use a method that allows several points to be plotted and an ROC curve to be fitted to them. Such a method, called the rating-scale method, is made possible by giving the observer more than two response alternatives, which allows the observer to adopt several threshold criteria simultaneously. This is done by asking the observer to rate each test during which a signal might have been presented on a four-point rating scale; for example--

0 - Confident, signal absent

1 - Less confident, signal absent

2 - Less confident, signal present

3 - Confident, signal present

Such a four-point rating scale gives three points on an ROC curve. If these are plotted on normal-normal probability paper, a best-fit line may be drawn and d' obtained from the graph.

PROBABILITY OF DETECTION ESTIMATES

Recognition Differential Method

In an actual mine emergency situation, many factors influence the chances of rescuing the miners, including time of arrival of the rescue team, life expectancy of the miners, search times, and operation time of the underground transmitter. This report has not discussed these points but rather has investigated the detection probability for an existing signal being measured by a rescue team in an area that in general is directly over a trapped miner. Even within this measurement, there are factors such as geology, noise, and depth that influence the probability of success. Although these factors preclude our stating the success of this measurement in a deterministic manner, we can, as outlined in this paper, quantify our chances in a probabilistic framework.

The probability of detection curve in figure 27 actually represents a conditional probability; that is, the likelihood that detection will occur given the presence of a fixed RMS SNR. As a consequence, the chance of detecting a signal transmitted through the earth can be calculated according to

$$P(D \text{ and } R_K) = P(R_K) \times P(D|R_K), \quad (2)$$

where $P(D \text{ and } R_K)$ represents the probability of achieving an SNR of size R_K and also detecting the signal in the noise. $P(R_K)$ is the probability of the occurrence of an SNR of size R_K, and $P(D|R_K)$ is the conditional probability of detecting a signal given an SNR of size R_K.

Figure 27 gives $P(D|R_K)$, and figures 19 through 22 show the SNR probability distributions. The latter figures show that these probabilities depend on frequency and depth. Using additional subscripts to account for these parameters, the probability of acheiving an SNR of size R_K and detecting the signal transmitted from a depth i at frequency j is

$$P_{ijk}(D \text{ and } R_K) = P_{ij}(R_K) \times P(D|R_K). \quad (3)$$

However, the primary result is the expected probability of detecting a signal transmitted at a specified depth for a known frequency summed over all possible R_K's. This is given as

$$P_{ij}(D) = \sum_{R_K} P_{ijk}. \quad (4)$$

These probability formulas and concepts can best be illustrated by a numerical example. For a transmission frequency of 3,030 Hz at an overburden depth of 1,000 ft, the data from table 2, also given in table 4, can be used with the results shown in figure 27 to obtain probability of detection for each SNR interval.

TABLE 4. - Detection probabilities

Signal-to-noise ratio interval, db	Probability of achieving signal-to-noise ratio in interval	Interval midpoint, db	Probability of detection at midpoint
Less than -3.....	0.3314	Less than -3	0.00
-3 to 0.....	.0804	-1.5	.00
0 to 3.....	.0843	1.5	.00
3 to 6.....	.0845	4.5	.15
6 to 9.....	.0809	7.5	.85
9 to 12.....	.0740	10.5	.99
Above 12.....	.2646	Above 12	1.00

Applying the summation formula, equation 4, the expected probability of detection at 1,000 ft and a frequency of 3,030 Hz is estimated to be--

$$P_{1,000,\ 3,030} = (0.3314)\ (0) + (0.0804)\ (0) + (0.0843)\ (0.01)$$
$$+ (0.0845\ (0.15) + (0.0809)\ (0.85)$$
$$+ (0.0740)\ (0.99) + (0.2640)\ (1.00)$$
$$= 0.43$$

The interpretation of this quantity is that a signal transmitted at 3,030 Hz through an overburden depth of 1,000 ft has a 43-pct probability of being detected on the surface in the general area above the transmitter when using the recognition differential method of observer detection.

Figure 30 shows the extension of these calculations to other frequencies and depths.

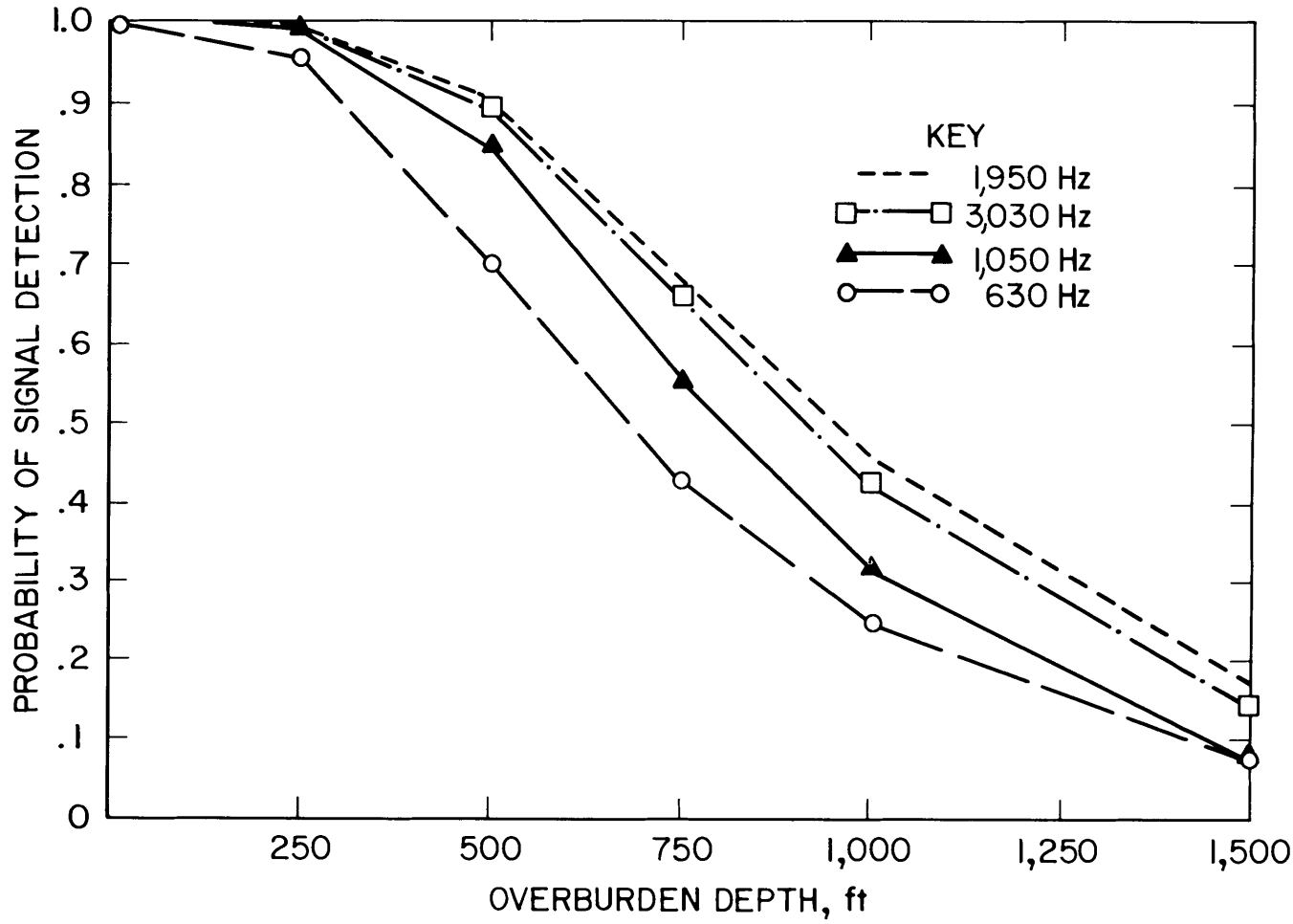

FIGURE 30. - Predicted probability of signal detection versus overburden depth by frequency for the GI transmitter as found by the recognition differential method.

Receiver Operating Characteristic Method

In work by Ristenbatt (11) tests were performed to verify the signal detectability performance of the present system. Tests were done using nine observers and the actual transmitter and receiver. The signal from the transmitter was mixed with wideband white noise and entered into the receiver at input SNR of 0 db, 3 db, and 6 db. The acoustic output of the receiver was then connected to a headset worn by the observer. Each observer was exposed to a series of 100 trials at each input SNR. Each trial lasted for 15 sec. After each 15-sec period, the observer chose one of four scaled responses as discussed earlier as the rating scale method.

These data were then used to determine the expected probability of detection (P_D) and probability of false alarm (P_{FA}) at the different SNR's. This testing provides the ROC for the present receiver, and the results are shown in figure 31. The shaded area around SNR of 0 and 6 db shows the variability in the data obtained. The variability around the SNR = 3 db wave is similar to that of the 0-db curve but is not shown in the interest of retaining clarity in the figure. Therefore, for a particular input SNR and preassigned P_{FA}, it is possible to determine the expected P_D of the observer.

The practical effect of false alarms is increased delay due to search time. Hence, false alarms are important not only for comparing different receivers but also in understanding the practical impact a receiver may have in a search and find mission.

It is the opinion of the author that an acceptable operating point for the false alarms of this system would be

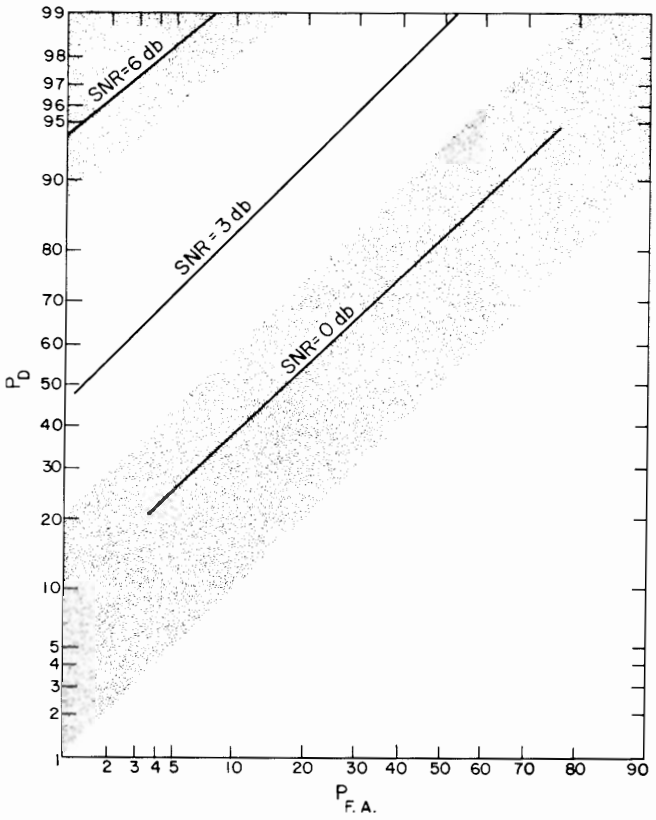

FIGURE 31. - Receiver operating characteristic curve for the trapped-miner receiver.

P_{FA} = 0.10. At this P_{FA}, figure 31 shows the expected P_D for the observer for different input SNR's.

It is now possible to recalculate the probability of detecting the trapped miner's signal based upon the ROC of the receiver. This work is similar to the method followed in the previous section, but the detection probabilities of the observer, based upon the recognition concept, are replaced by that of the ROC method and the data obtained by way of figure 31.

These results are shown in figure 32 and show a slight improvement over those shown in figure 30.

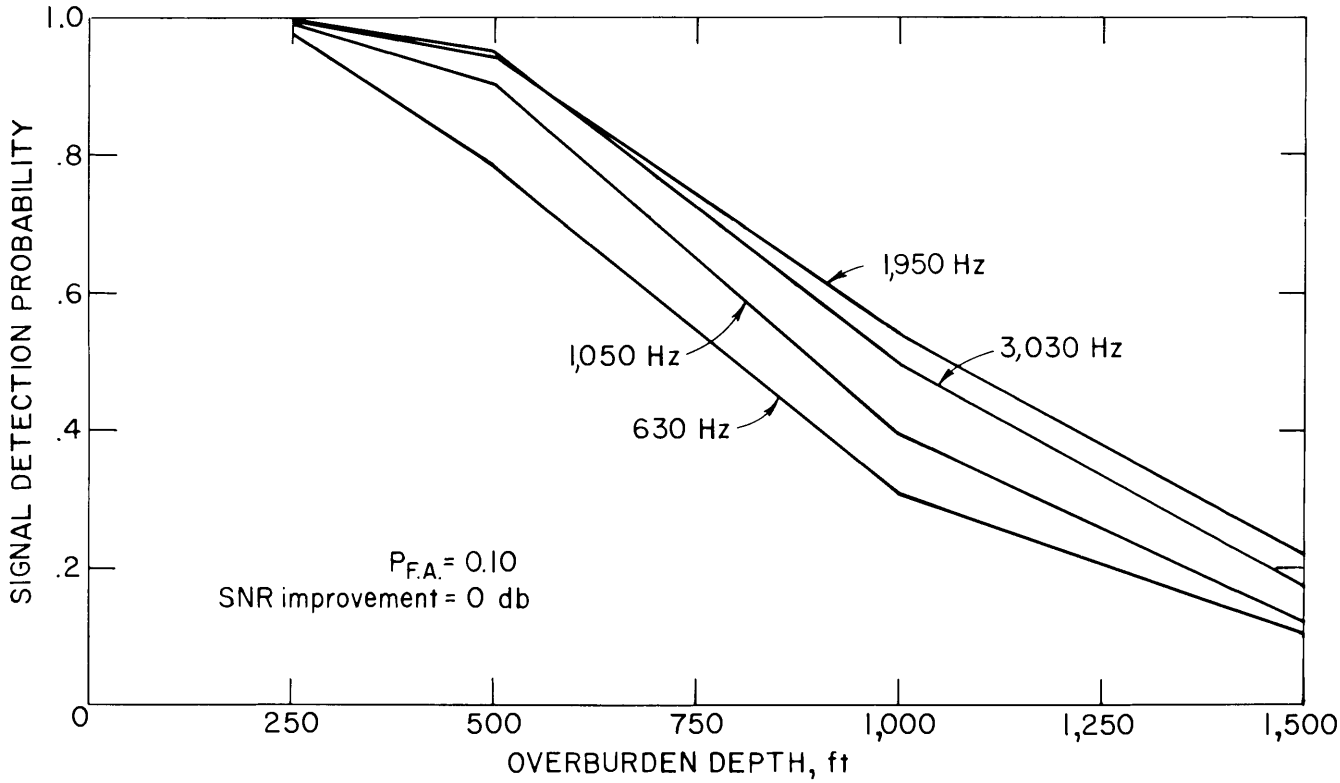

FIGURE 32. - Predicted probability of signal detection versus overburden depth by frequency for the GI transmitter as found by the ROC method.

SENSITIVITY ANALYSIS

It is informative to observe the amount of increase in signal detectability for increases in SNR of the trapped-miner signal on the surface of the mine.

Figures 33, 34 and 35 show the expected probability of detection as the expected SNR is improved over that found from the field tests for values of +3 db, +6 db, and +12 db. As expected, the probabilities increase greatly, going from 54 pct for no SNR improvement at 630 Hz and 1,000 ft to 84 pct for +12 db SNR improvement.

Additional insight is provided by way of figure 36, where the detection probabilities are shown for each frequency at a depth of 1,000 ft as the SNR is improved. To obtain a detection probability of 90 pct at 1,000 ft, a frequency of 1,950 would be used and an SNR improvement of approximately 18 db would be needed. A rough estimate shows that for all frequencies the probability of detection increases between 6 and 8 pct at 1,000 ft for every 3-db improvement in SNR.

Various areas of investigation may be studied to acquire larger SNR. The obvious first choice is to increase the strength of the signal source. However, inherent constraints due to intrinsic safety considerations would limit any gain by this technique to only a few decibels. Correlation techniques could be used where an array of receiving antennas could improve detectability. This is the objective of a current project (14). Incoherent integration of the present signal has been suggested by Ristenbatt (12) and is the technique proposed by General Instrument Corp. (6) in an adaptation to the present receiver.

Noise cancellation through correlation techniques involving the noise at the

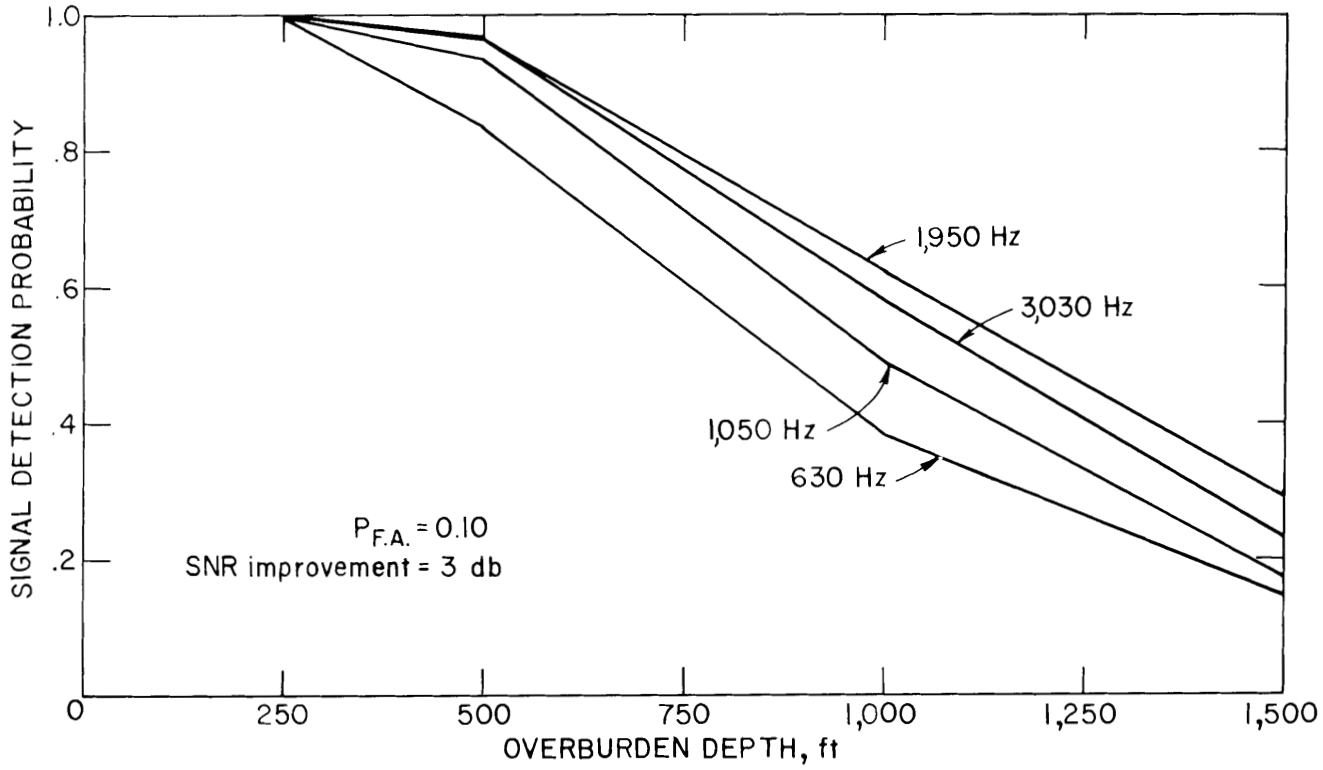

FIGURE 33. - Predicted probability of signal detection versus overburden depth by frequency for the GI transmitter as found by the ROC method with a 3-db SNR improvement.

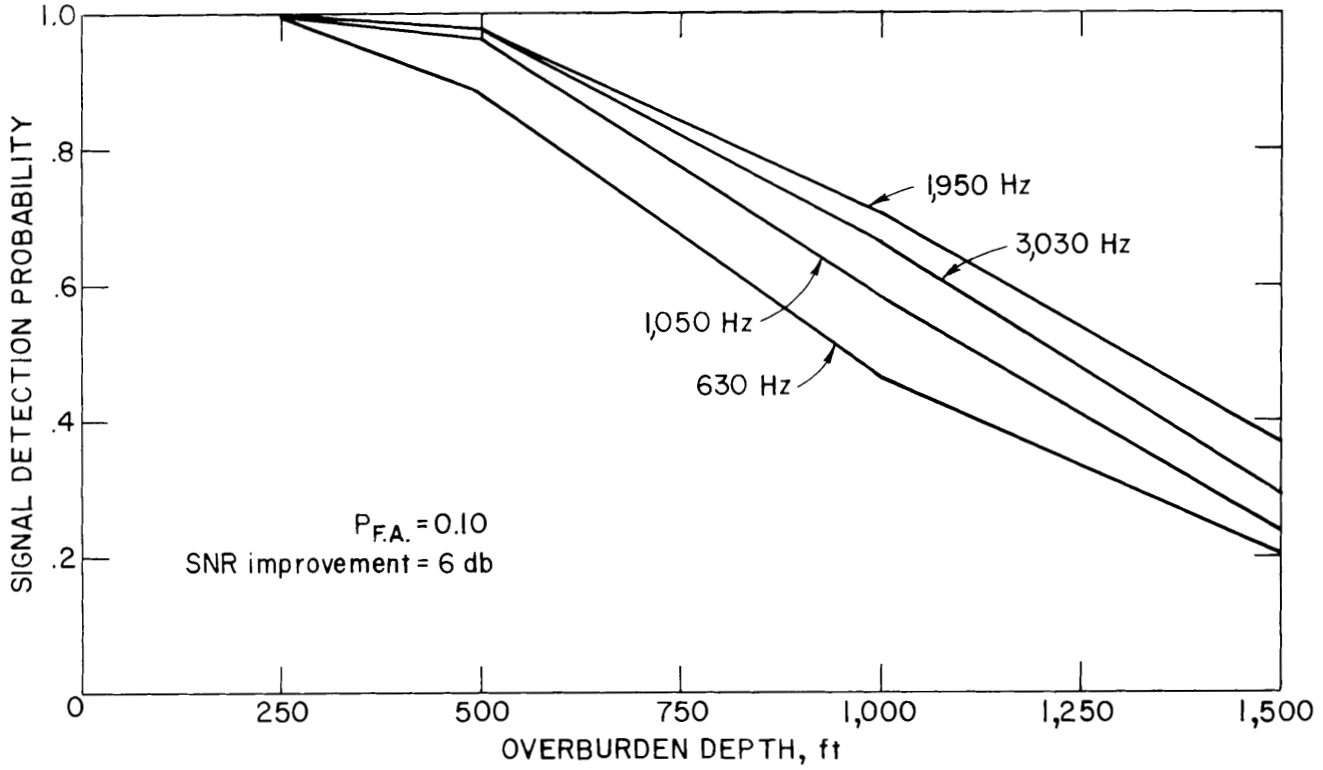

FIGURE 34. - Predicted probability of signal detection versus overburden depth by frequency for the GI transmitter as found by the ROC method with a 6-db SNR improvement.

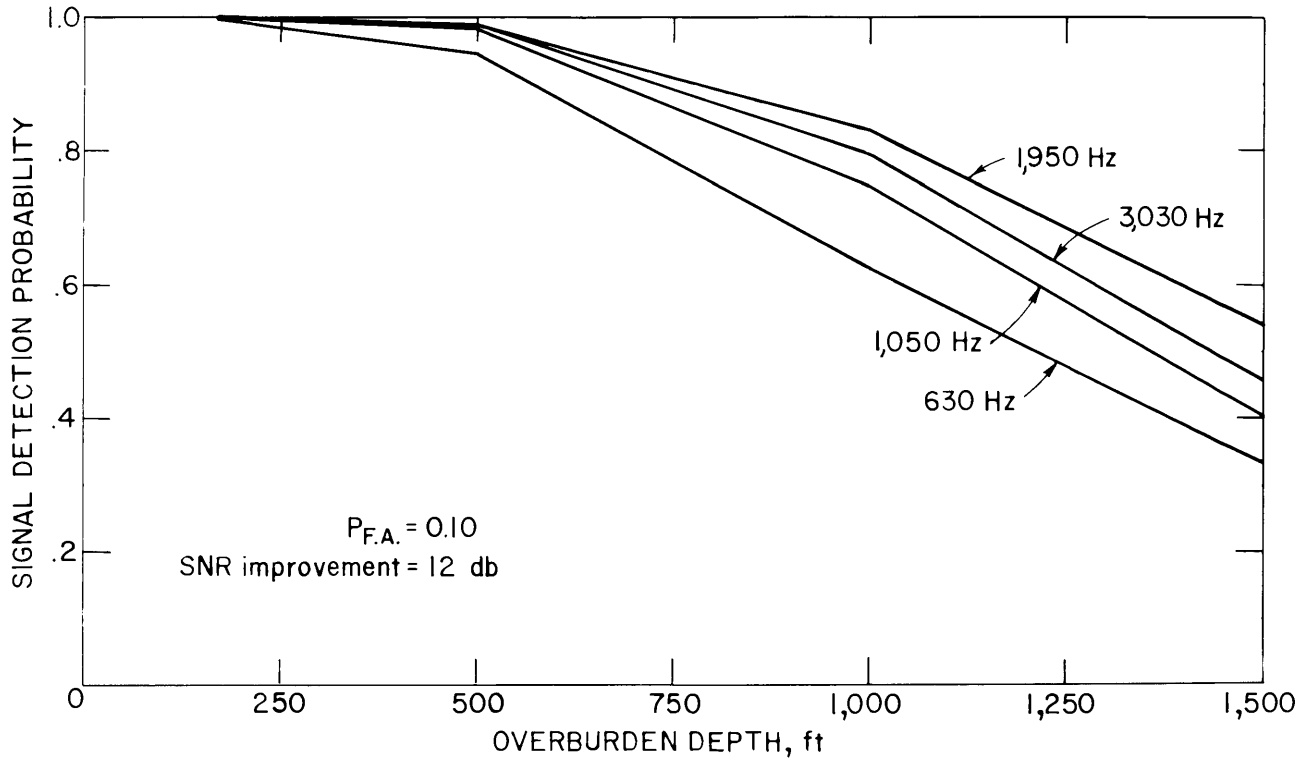

FIGURE 35. - Predicted probability of signal detection versus overburden depth by frequency for the GI transmitter as found by the ROC method with a 12-db SNR improvement.

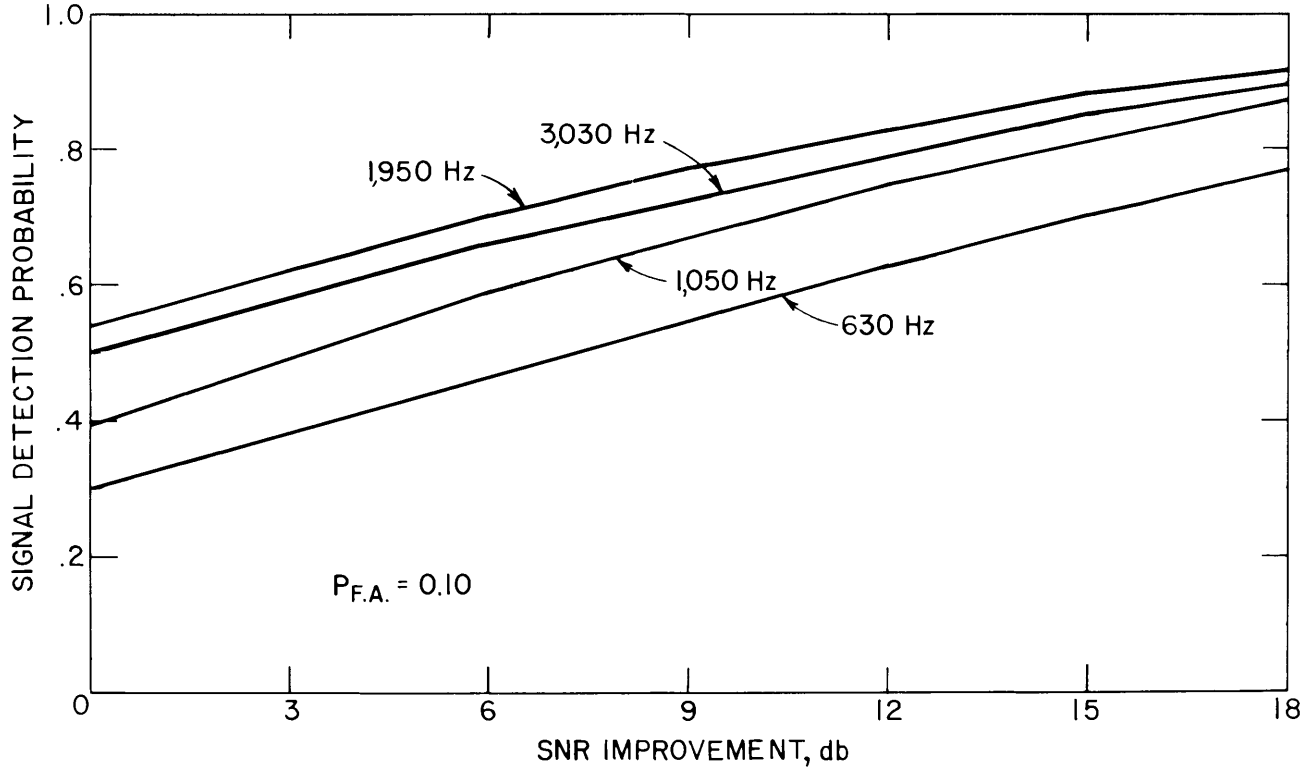

FIGURE 36. - Predicted probability of signal detection versus SNR improvement by frequency for the GI transmitter for a mine depth of 1,000 ft.

receiving antenna and a distant antenna outside the signal's range is an area for future study.

The parameters of the signal that affect an observer's ability to detect a pulsed continuous wave (CW) signal in noise, discussed earlier, could be studied to improve detectability. However, these studies must also be conscious of the efficient use of the power of the transmitter battery and of schemes used in search procedures.

Possibly the most promising venture to improve signal detectability is a project under investigation by Develco (2). Here, the underground transmitter is similar to the one discussed in this report except that the signal is not pulsed, but rather transmitted continuously. The surface receiver is a microcomputer which coherently integrates the transmitted signal. The principal idea is to exchange time for signal detectability. The receiver continually monitors the signal, and if it exists and is within the detectable range of the receiver, it will eventually be detected. This system was originally designed to detect signals transmitted from a depth of 3,000 ft and should be able to easily detect signals at a depth of 1,000 ft in a few minutes of operation. Location is performed by vector calculation of the signal at a number of receiving-antenna locations.

SUMMARY

This paper has discussed the results of an extensive field-testing program to evaluate the performance of the EM trapped-miner transmitter. Analysis of these data has enabled one to place into a probabilistic framework the ability to confidently detect the signal from the underground transmitter. Two methods have been used to determine the probability of signal detection. The first, known as the recognition differential method, has indicated that the probability of signal detection at a depth of 1,000 ft is 45 pct; at 500 ft it is 90 pct. These depths exceed the actual depths of 90 pct and 50 pct, respectively, of U.S. coal mines.

The second method, which is preferred to the former, is known as the receiver operating characteristic method. This method relates both signal detectability and false alarm rate. Using this method, it was found that for a 10-pct false alarm rate the probability of detection at 1,000 ft and 500 ft is 54 and 95 pct, respectively. This information is vital for the future formulation and promulgation of new regulations written for the use of the EM system. Studies are underway to improve the detection capability by providing signal-processing capability to the receiver. Future work will look at a systems approach when using this technique. This study will investigate each element involved in a successful rescue effort, such as search strategies and life expectancies. Coupled with the results discussed in this paper, a thorough understanding of the effective implementation of the EM system should be obtained.

REFERENCES

1. Collins Radio Group. Waveform Generator--Package and Receivers. Final Report for BuMines Contract HO242010, April 1977, 14 pp.; available for consultation at Pittsburgh Research Center, Bureau of Mines, Pittsburgh, Pa.

2. Develco. EM Rescue System for Deep Mines. BuMines Contract J0199009, May 1979; available for consultation at Pittsburgh Research Center, Bureau of Mines, Pittsburgh, Pa.

3. Durkin, J., and R. Greenfield. Evaluation of the Seismic System for Locating Trapped Miners. BuMines RI 8567, 1981, 55 pp.

4. Garner, W. R. Auditory Thresholds of Short Tones as a Function of Repetition Rates. J. Acoustical Soc. America, v. 19, No. 4, July 1947, pp. 600-608.

5. General Instrument Corp. Design to Specification and Fabrication of VF Transmitters and Baseband Receivers. BuMines Contract J0395917, December 1978; available for consultation at Pittsburgh Research Center, Bureau of Mines, Pittsburgh, Pa.

6. _____. Proposal To Improve Detection Capability of Trapped Miner EM Receiver. Proposal QR 9067, March 1980; available for consultation at Pittsburgh Research Center, Bureau of Mines, Pittsburgh, Pa.

7. Lagace, R., J. Dobbie, T. Doerfler, W. Hawes, and R. Spencer. Technical Support of Through-the-Earth Transmission Measurement. Arthur D. Little Inc., Final Report for BuMines Contract J0188037, June 1980, 188 pp.; available for consultation at Pittsburgh Research Center, Bureau of Mines, Pittsburgh, Pa.

8. National Academy of Engineering, Committee on Mine Rescue and Survival Techniques. Mine Rescue and Survival, Final Report-BuMines OFR 4-70, March 1970, 81 pp.; available for consultation at the Bureau of Mines facilities at Denver, Colo., Minneapolis, Minn., Pittsburgh, Pa., Juneau, Alaska, and Spokane, Wash.; at the MSHA facilities at Pittsburgh., Pa., Wilkes-Barre, Pa., Johnston, Pa., St. Clairsville, Ohio, Mount Hope, W. Va., Morgantown, W. Va., and Norton, Va.; and at the National Library of Natural Resources, U. S. Department of the Interior, Washington, D.C.

9. National Defense Research Committee (NDRC) Division 6. Principles and Applications of Underwater Sound, Summary Technical Report. Washington, D.C., v. 7, 1947 (revised 1968).

10. Peterson, W., T. G. Birdsall, and W. C. Fox. The Theory of Signal Detectability. IRE Trans., 1954, pp. 171-212.

11. Ristenbatt, M. D. Post Disaster Communication Techniques. University of Michigan, Final Report for BuMines Contract J0199109, December 1980, 99 pp.; available for consultation at Pittsburgh Research Center, Bureau of Mines, Pittsburgh, Pa.

12. _____. Personal Correspondence, February 3, 1980; available for consultation at Pittsburgh Research Center, Bureau of Mines, Pittsburgh, Pa.

13. Swets, J. A. (ed.) Signal Detection and Recognition by Human Observers. John Wiley & Sons, New York, 1964, 702 pp.

14. University of Pittsburgh. A Study for the Detection of Weak Electromagnetic Signal Bursts With Hard-Limited Arrays. BuMines Contract J0318033, December 1980; available for consultation at Pittsburgh Research Center, Bureau of Mines, Pittsburgh, Pa.

15. Urick, R. J. Principles of Underwater Sound for Engineers. McGraw-Hill Book Co., Inc., New York, 1967, 450 pp.

16. Wait, J. Subsurface Electromagnetic Fields of a Circular Loop of Current Located Above the Ground. IEEE Trans. on Antenna and Propagation, July 1972, pp. 520-522.

17. Westinghouse Corp. Reliability and Effectiveness Analysis of the USBM Electromagnetic Location System for Coal Mines. Final Report for BuMines Contract J0166060, December 1978, 151 pp.

☆U.S. GOVERNMENT PRINTING OFFICE: 1982 - 505 - 002/76 INT.-BU.OF MINES,PGH.,PA 26339